# Nanostructured Hafnium Oxide based Noninvasive Biosensor for Oral Cancer Detection

*A major project dissertation submitted*

*in partial fulfilment of the requirement for the degree of*

**Master of Technology**

**In**

**Biomedical Engineering**

*Submitted by*


**SACHCHIDANAND TIWARI**

**(2K13/BME/20)**

**Delhi Technological University, Delhi, India**


*Under the supervision of*

Prof. Bansi D. Malhotra


Department of Biotechnology
Delhi Technological University
Delhi-110042, INDIA

# DECLARATION

Certified that the project report entitled **"Nanostructured Hafnium Oxide based Noninvasive Biosensor for Oral Cancer Detection"** submitted by me is in partial fulfilment of the requirement for the award of the degree of Master of Technology in Biomedical Engineering, Delhi Technological University. It is a record of original research work carried out by me under the supervision of **Prof. Bansi. D. Malhotra**, Department of Biotechnology, Delhi Technological University, Delhi.

The matter embodied in this project report is original and has not been submitted for the award of any Degree/Diploma.

**Date:**

**Sachchidanand Tiwari**
(2K13/BME/20)
Department of Biotechnology
Delhi Technological University
Delhi-110042.

# CERTIFICATE

This is to certify that the major project entitled **"Nanostructured Hafnium Oxide based Noninvasive Biosensor for Oral Cancer Detection"** submitted by **Sachchidanand Tiwari (2K/13/BME/20)** in partial fulfilment of the requirement for the award of the degree of Master of Technology in Biomedical Engineering, Delhi Technological University, is an authentic record of the candidate's own work carried out by him under my supervision. The information and data enclosed in this dissertation is original and has not been submitted elsewhere for honouring of any other degree.

**Date:**


**Prof. D. Kumar**
Head
Department of Biotechnology
Delhi Technological University
Delhi-110042.

**Prof. Bansi D. Malhotra**
Project Mentor
Department of Biotechnology
Delhi Technological University
Delhi-110042.

# ACKNOWLEDGEMENT

*First and fore-most I bow down to the divine almighty for providing me inspiration, support and constant strength to achieve this milestone which can add meaning to my life.*

*This dissertation report would not have been possible without the generous help from many people. First of all, I would like to express my profound sense of reverence of gratitude to my mentor* ***Prof. Bansi D. Malhotra****, Department of Biotechnology, Delhi Technological University, for his valuable guidance, congenial discussion, incessant help, calm, endurance, constructive criticism and constant encouragement throughout this investigation right from the imitation of work to the ship shaping of manuscript.*

*I express my kind regards and gratitude to* ***Prof. D. Kumar****, (HOD, Department of Biotechnology), and all faculty members for helping in my project.*

*I am highly indebted to* ***Mr. Suveen Kumar*** *and* ***Mr. Saurabh Kumar*** *(Research Scholar) for their guidance and constant supervision as well as for providing necessary information regarding the instruments and experiments and also for their support in completing the report. I am highly grateful to* ***Ms. Shine Augustine*** *and* ***Dr. Saurabh Shrivastava*** *for their valuable suggestions and guidance during the entire tenure of my dissertation work.*

*I would also like to thanks* ***Mr. Chhail Bihari****,* ***Mr. Jitendra Singh*** *and* ***Mr. Mukesh Kumar*** *for providing necessary chemicals and maintaining laboratory in good condition.*

*At last but never the least, words are small trophies to express my deep sense of gratitude and affection to my loving friend and my parents who gave me infinite love to go for this achievement.*

*(SACHCHIDANAND TIWARI)*

# CONTENTS

# LIST OF ABBREVIATIONS

| | |
|---|---|
| Ab | Antibody |
| APTES | 3-Aminopropyltriethoxysilane |
| AgCl | Silver chloride |
| BSA | Bovine serum albumin |
| CE | Counter electrode |
| DI | DI |
| DNA | Deoxyribonucleic acid |
| $E_{pa}$ | Anodic peak potential |
| $E_{pc}$ | Cathodic peak potential |
| EDC | N-ethyle-N'-(3-dimethylaminopropyl) carbodiamide |
| FET | Field-effect-transistor |
| HRP | Horseradish peroxidise |
| $I_{pa}$ | Anodic peak current |
| $I_{pc}$ | Cathodic peak current |
| ITO | Indium-tin-oxide |
| NHS | N-hydroxysuccinimide |
| nMOx | Nanostructured metal oxides |
| RSD | Relative standard deviation |
| SAM | Self-assembled monolayer |
| SPR | Surface Plasmon resonance |
| V | Volt |
| $ZrO_2$ | Zirconium oxide |

# LIST OF TABLES

# LIST OF SCHEMES/FIGURES

# Chapter-1

# Abstract

# Nanostructured Hafnium Oxide based Noninvasive Biosensor for Oral Cancer Detection

Sachchidanand Tiwari

Delhi Technological University, Delhi, India
E-mail ID: tiwari.biotech11@gmail.com.

## 1. Abstract

This dissertation contains results of the studies relating to fabrication of the non-invasive and label free, novel nanostructured immunosensor platform (BSA/anti-CYFRA-21-1/APTES/$HfO_2$/ITO) for efficient detection of an oral cancer biomarker (CYFRA-21-1) in saliva. Nanostructured hafnium oxide has been synthesized via one step low temperature hydrothermal process and surface modified with 3-aminopropyltriethoxy silane (APTES) for covalent immobilization of monoclonal anti-CYFRA-21-1. Structural, morphological and spectroscopic characterization of the fabricated electrodes have been carried out using X-ray diffraction (XRD), transmission electron microscopy (TEM), X-ray photoelectron spectroscopy (XPS) and fourier transform infrared spectroscopy (FT-IR). The results of the response studies reveal that the BSA/anti-CYFRA-21-1/APTES/$HfO_2$/ITO immunoelectrode can be used to estimate the CYFRA-21-1 with a high sensitivity of 9.28 µA mL $ng^{-1}$ $cm^{-2}$, has a wide linear detection range (LDR) of 2-18 ng $mL^{-1}$, limit of detection (LOD) as 0.209 ng $mL^{-1}$ and shelf life of 8 weeks. Further, the sensing results obtained using this immunosensor have been validated with enzyme linked immunosorbent assay (ELISA) in saliva samples of oral cancer patients. The improved biosensing characteristics of the fabricated hafnium oxide based immunoelectrode reveal that this platform can be efficiently utilized for the fabrication of noninvasive point of care device for oral cancer monitoring.

# Chapter-2

# Introduction

## 2. Introduction

Oral cancer, caused due to uncontrolled growth of cells in the mouth, is currently the sixth most common cancer.(Kujan et al. 2006) There is thus an increased demand for diagnosis, prognosis and for treatment of this dreaded disease.(Brocklehurst et al. 2013) If undetected at an early stage, the cancer metastasizes in the rest of the body parts leading to death. Thus, diagnosis of the oral cancer at an early stage as well as planning of the appropriate treatment is highly desirable.(Brocklehurst et al. 2013; Malhotra et al. 2012) The conventional methods such as laser capture microdissection, visualization adjuncts, cytopathology and biopsies currently being used for detection and monitoring of the oral cancer are expensive, labor-intensive, time consuming and require serum/blood.(Malhotra et al. 2012; Mehrotra and Gupta 2011; Rosenberg and Cretin 1989; Scully et al. 2008) Therefore, there is an urgent requirement for availability of a new technique for rapid identification of oral cancer. In this context, biosensors have been considered as an attractive and cost-effective technique for the detection of oral cancer.(Arya and Bhansali 2011; Chen et al. 2011; Kumar et al. 2011; Malhotra et al. 2012; Malhotra et al. 2010) Among the various biosensors, electrochemical (EC) biosensors are considered promising bioanalytical devices offer high sensitivity, improved detection limit, multianalyte detection, automation, require small sample volume and are not affected by sample turbidity.(Malhotra et al. 2010; Mehrotra and Gupta 2011; Wang 2006) Besides this, they require relatively simple instrumentation that requires low-power and can be easily miniaturized.(Arya and Bhansali 2011; Kumar et al. 2013)

The identification of biomarkers is considered important for OC detection. Some of the important biomarkers in oral cancer detection are interleukin-8 (IL-8), interleukin-6 (IL-6), vascular endothelial growth factor (VEGF) and epidermal growth factor receptor (EGFR).(Chen et al. 2011; Li and Yang 2011; Malhotra et al. 2010; Mehrotra and Gupta 2011; Yang et al. 2005) These biomarkers are secreted in biological fluids in very low amount (~pg $mL^{-1}$) and hence require testing via ultrasensitive detection strategies. These biomarkers are secreted in serum/blood samples and hence are invasive.(Chen et al. 2011; Li and Yang 2011; Malhotra et al. 2010; Wang et al. 2013b; Yang et al. 2005). Detection via salivary biomarkers is a promising non-invasive approach for early detection of oral cancer and has become an area of increased research interest in recent years.(Rajkumar et al. 2015; Scully et al. 2008) In this context, CYFRA-21-1 has been found to be over-secreted in saliva. In normal subjects level of CYFRA-21-1 is found to be 3.8 ng $mL^{-1}$ whereas in patients suffering from oral cancer it increases to $17.46 \pm 1.46$ ng $mL^{-1}$.(Nagler et al. 2006; Rajkumar et al. 2015) Keeping this in view, a painless and noninvasive electrochemical biosensor based on nanostructured zirconia has recently been reported for the detection of CYFRA-21-1 in saliva samples.(Kumar et al. 2015)

The performance of an EC biosensor is known to depend on the physiochemical properties of the material and biomolecules immobilized onto an electrode.(Arya and Bhansali 2011; Kumar et al. 2013; Wang 2006) Direct immobilization of antibody onto an electrode surface requires materials with large surface-to-volume ratio, biocompatibility and ease of surface modification.(Ali et al. 2013; Arya and Bhansali 2011; Solanki et al. 2011) Nanostructured metal oxides have recently been found to exhibit interesting nanomorphological, functional, biocompatible and catalytic properties and are thus promising materials for biomolecules immobilization since they offer effective surface with desired orientation, better conformation and high biological activity resulting in enhanced biosensing

characteristics.(Solanki et al. 2011; Vasudev et al. 2013) Hafnium (atomic number 72) is a tetravalent transition metal present in IV$^{th}$ group. Nanostructured hafnium oxide is an attractive inorganic metal oxide comprising of hafnium and oxygen elements. It can be prepared using soft chemistry i.e. one step low temperature hydrothermal process and sol-gel process.(Chaubey et al. 2012; Fahrenkopf et al. 2012) It exhibits high surface to volume ratio, thermal stability, chemical inertness, non-toxicity, and affinity for groups containing oxygen that make it an interesting material for biosensing application.(Chaubey et al. 2012; Liu et al. 2010; Michael et al. 2014) The isoelectric point of hafnium oxide is 7.0 that makes its surface neutral at physiological pH. Furthermore, oxygen moieties in $HfO_2$ can help to facilitate covalent attachment of linker molecules that can be useful for immobilization of biomolecules.(Das et al. 2011; Fahrenkopf et al. 2012; Lee et al. 2012; Shim et al. 2013) Lee et al. have proposed an invasive biosensor based on hafnium oxide for detection of human interleukin-10.(Lee et al. 2012)

This dissertation contains results of studies relating to the fabrication of nanostructured hafnium oxide based immunosensor based on anti-CYFRA-21-1 for detection of oral cancer in saliva samples. Efforts have also been made to investigate the structural, optical and spectroscopic characterization of anti-CYFRA-21-1 immobilized nanostructured hafnium oxide electrode. To the best of our knowledge, this is the first report on the application of nanostructured hafnium oxide based immunoelectrode for oral cancer detection.

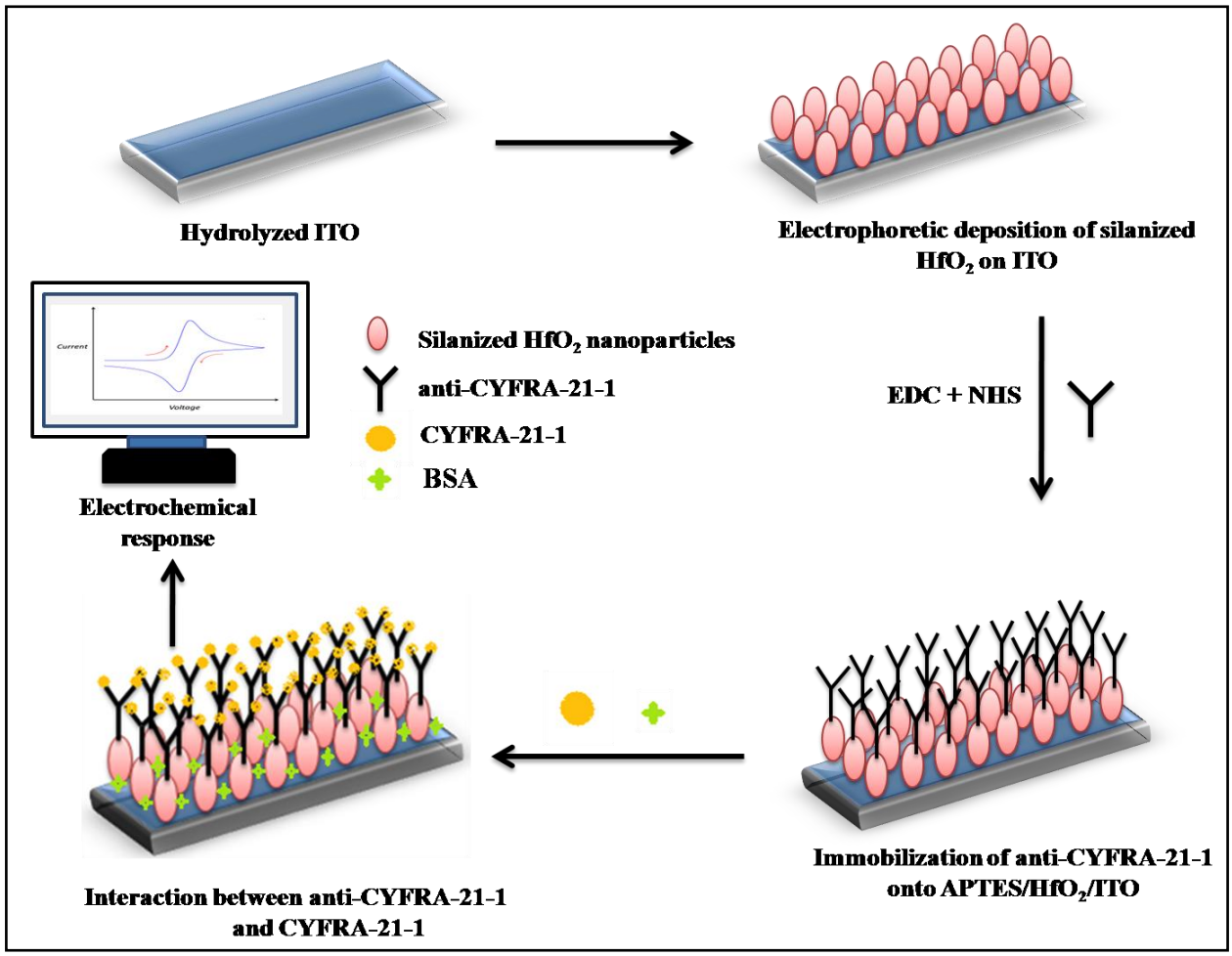


**Scheme 1:** Fabrication steps of BSA/anti-CYFRA-21-1/APTES/$HfO_2$/ITO platform for oral cancer detection.

# Chapter-3

# Literature review

## 3.1. Oral cancer

All malignancies originating in oral or mouth cavity are known as oral cancer (OC). OC appears as uncontrolled growth or sore in the mouth cavity that does not heal. OC includes cancer of the lips, cheeks, tongue, floor of the mouth, hard and soft plate, sinuses and pharynx (throat).(Kademani 2007) Squamous cell carcinoma, which develops in the tissue that lines the mouth and lips or in lining of oral mucosa independently accounts for over 90% of OC.(Massano et al. 2006)

OC most commonly developed in older and middle aged individuals, but in recent years a large number of younger adults found with these malignancies.(Silverman 2003) OC can be divided into three categories on the basis of epidemiological and clinicopathological perspective: carcinomas of oral cavity, carcinomas of oropharynx and carcinomas of lips. Oropharyngeal malignancies are more common among male than female, with ratio of over 2:1. In contrast to oropharyngeal malignancies, carcinomas of the lips are more epidemiologically similar to squamous cell carcinomas of the skin and found primarily in men. These malignancies are strongly associated with chronic sun exposure although these carcinomas sometimes related to the specific site of the lips where cigarettes or other means of tobacco smoking habitually held.(Zini et al. 2010)

The strong association between tobacco use and OC is well established. The risk of developing OC is 5-9 times greater for smokers in comparison to non smokers, and this risk may increase to as much as 17 times greater for extremely heavy smokers of 80 or more cigarettes per day.(Proia et al. 2006) Approximately 80% of the OC patients are the smokers which is two to three times greater than general OC (non smoker) patients. In addition, treated oral cancer patients who continue to smoke have a two to six times greater risk of developing a second malignancy of the upper aero digestive tract than those who stop smoking.(Graham et al. 1977) The use of Marijuana is also considered to be a potential risk factor responsible for the developing OC in younger adults.(Firth 1997)

Snuff and chewing tobacco have also been associated with an increased risk for oral cancer. In addition, a significant number of oral cancers in smokeless tobacco users develop at the site of tobacco placement. Consumption of smoked tobacco associated with much higher cancer risk in comparison to smokeless tobacco.(Proia et al. 2006)

Alcohol consumption has been identified as a major risk factor for OC. In studies controlled for smoking, moderate-to-heavy drinkers have been shown to have a 3-9 times greater risk of developing OC.(Llewellyn et al. 2004) Patients who are both heavy smokers and heavy drinkers can have over one hundred times greater risk for developing a malignancy.(Graham et al. 1977) Other factors include poor nutrition, poor oral hygiene and some chronic infection caused by bacteria and viruses are responsible for OC.(Graham et al. 1977; Kademani 2007)

Recent studies suggest that some strains of human papillomavirus (HPV) may be associated with some oral and oropharyngeal cancers. HPV-16 and HPV-18 has been detected in up to 22 % and 14 % respectively in OC cases.(Herrero et al. 2003) Anaemia, iron deficiency in combination with dysphagia and esophageal webs (Plummer Vinson or Paterson-Kelly syndrome) is associated with an elevated risk for development of OC.(Zini et al. 2010) Immunosuppression appears to predispose some individuals to an increased risk for oral cancer.(Silverman 2003)

Symptoms of OC may include red, white and/or a mixture of these colors in patches, a non-healing sore on the face, neck and mouth or lips, pain and tenderness in any area of mouth, bleeding in mouth, loose teeth, chewing and swallowing difficulties, and change in voice.(Firth 1997; Graham et al. 1977; Kademani 2007; Silverman 2003)

## 3.2. Conventional methods for detection of oral cancer

Many studies have been made in recent years to improve cancer diagnosis and prognosis throughout the body, but the diagnosis and prognosis of the OC has not experienced similar improvement.(Lestón and Dios 2010) Because five-year survival is directly related to stage at diagnosis, prevention and early detection efforts have the potential not only for decreasing the incidence, but also for improving the survival of those who develop this disease. Unfortunately, most patients are diagnosed with advanced stage (stage 3 and 4) disease.(Kujan et al. 2006) Early detection, therefore, needed to improve survival rate as well as access to oral health services for all mankind.

Conventional oral visualization, biopsy, histopathology and palpation examination constitutes the standard screening methods for OC.(Fedele 2009; Lestón and Dios 2010; Mehrotra et al. 2006; Mehrotra and Gupta 2011) There are also a number of methods that may variously contribute to the diagnosis of OC,(Patton et al. 2008) some of them are given below;

- **Light based diagnostic methods:-** In recent years a number of light-based methods have been developed for the earlier detection of OC. These methods are used as optional to the conventional mouth cavity examination to help visualize lesions.(Fedele 2009; Scully et al. 2008) These methods mainly based upon the absorbance difference of the abnormal metabolite and structure changes of cells.
- **Cytological Techniques:-** Different methods of cell biology and molecular biology to study phenotypes and cellular functions of tissues or cells come under the cytological techniques..(Mehrotra and Gupta 2011)
- **Brush Biopsy:-** In this biopsy method, to collect the cells sample a bristled catheter is used into the suspected area of disease. This technique can be minimal invasive means to diagnose OC.(Brocklehurst et al. 2013) The major drawback associated with brush biopsy is that, by only means of visualization the OC is poorly identified.(Farah et al. 2012)
- **Vital staining:-** Toluidine blue (TB) is widely used staining toll for diagnose early OC. In this method 1% aqueous solution of TB applied to doubtful lesion for about 30 seconds.(Farah et al. 2012; Fedele 2009) After reaction time i.e. 30 seconds, acidophilic metachromatic nature of TB helps to differentiate areas of carcinomas. TB staining has been found to be highly sensitive method to diagnose OC but it also produces false negative results up to 58%, which makes it unsuitable technique for precancer detection.(Kujan et al. 2006; Lestón and Dios 2010)
- **Laser Capture Microdissection (LCM):-** LCM can be used to isolate carcinomas from microscopic regions of tissues or cells with preserved cell morphology.(Fend and Raffeld 2000) This technique has boosted the molecular study of cancer cells by providing more precise information on molecular level.(Lestón and Dios 2010) With the combination of immunohistochemical staining, we can obtain more accurate molecular information of cells. The use of SELDITOF-MS technology with LCM and bioinformatics, better molecular diagnostic results can be obtained.(Fend and Raffeld 2000)
- **Microscopy:-** The study of biochemical composition of the cell helps to diagnose the alteration in cell before the symptoms manifested morphologically.(Mehrotra et al. 2006; Wang et al. 1999) Spectral cytopathology (SCP) allow the collection of spectrum from an individual cell and detect internal biochemical changes arise due to disease.SCP works on

principles of vibrational spectroscopy for detection of intracellular biochemical changes.(Lestón and Dios 2010)

These methods are invasive, time-consuming, expensive, and labour-intensive. In this context, biosensors offer a reliable, user-friendly, increased assay speed, high sensitivity and require low sample volumes.(Kumar et al. 2015)

## 3.3. Biosensors

According to International Union of Pure and Applied Chemistry, biosensor is a self-contained integral device that is capable of providing specific quantitative or semi-quantitative analytical information using a biological element. In a biosensor, physio-chemical change produced by specific interactions between the target analyte and biological element is detected and is measured by a transducer. Biological element may be antibody, enzyme, receptor protein, nucleic acid, cell or tissue. In the past decade biosensing devices have aroused increasing interest in health care sector and environmental monitoring due to their high specificity, sensitivity, speed, portability and low cost.

## 3.4. Components of a biosensor

Biosensor has three major components: (i) a bio-recognition element such as enzyme, DNA, antibody etc. for recognition of an analyte also known as bio-receptor, (ii) an immobilization matrix such as conducting polymers, nanomaterials, sol– gel films, and self-assembled monolayers, which are used for the immobilization of a biomolecule and (iii) a transducer unit for conversion of biochemical reaction product into a recognizable signal **[Scheme 2]**. Bio-receptor and transducer together may also be referred as a biosensor membrane.

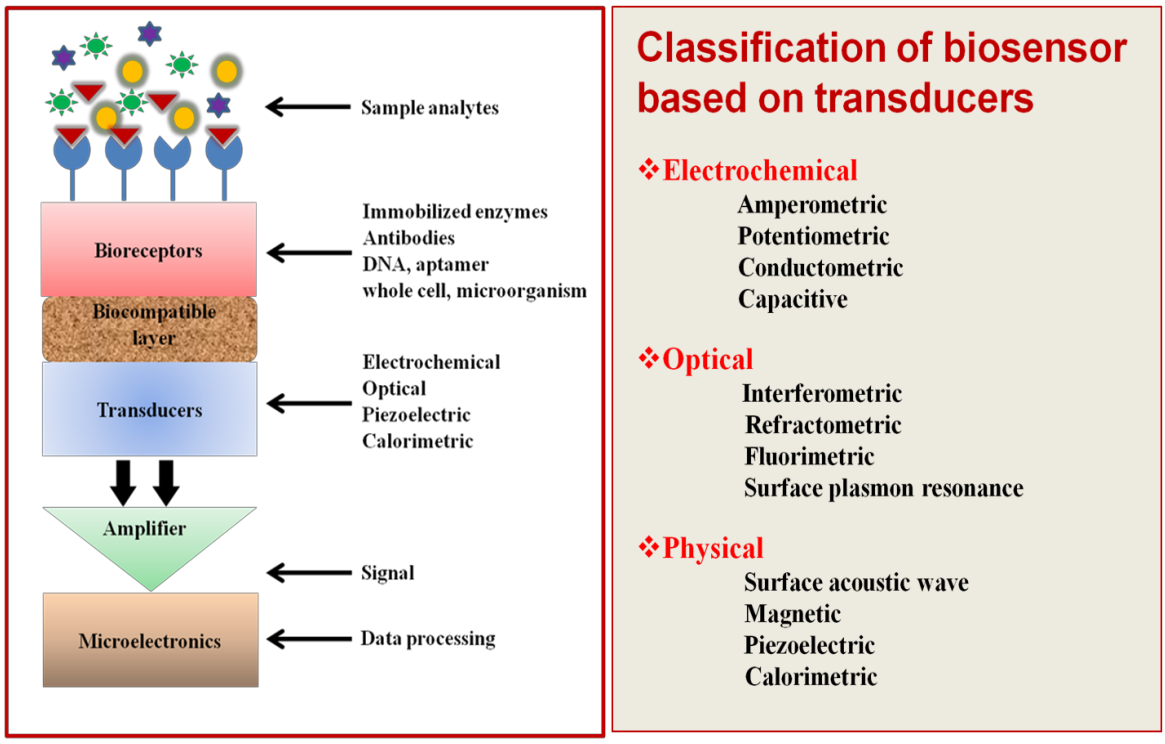


**Scheme.2**. Components and classification of biosensor.

### 3.4.1. Biomolecular recognition element

Biomolecular recognition element i.e., bioreceptor is a biomolecule or molecular assembly that has the capability of recognizing a target/substrate i.e. an analyte. The most commonly used bioreceptors in biosensors are enzymes, antibodies, DNA or whole cells. These bio molecular recognition elements having ability to recognize biomarkers secreted in body fluids such as blood, saliva, urine, sweat etc. Among these, blood is one of the prominent body fluid which is commonly used for detection of biomarkers. Use of blood sample in biomarkers recognition is invasive, high cost processing, require clinical expert for sample collection, handling, storage etc. make the overall process highly complex. To overcome these limitations saliva could be a promising candidate for biomarker detection or analysis.

Whole saliva is a colourless, watery and thick compound produced from the salivary glands. It comprises of 98% water and 2% other important substances including various enzymes, electrolytes, glycoproteins, blood constituents, viruses, bacteria, fungi, exfoliate cells and food debris.(Giannobile et al. 2009) The transport mechanism of proteins and ions from serum into salivary gland ducts has been shown in **Figure 1.**(Haeckel and Hanecke 1996) The ions present in saliva act as buffer to maintain the pH range from 6.2-7.4, which prevents minerals in dental hard tissues from dissolving. Because of salivary components such as glycoproteins, blood constituents and cell debris, it is a clinical informative tool for diagnosis and monitoring of various diseases.(Lee and Wong 2009)

Use of saliva as a diagnostic tool is an emerging field utilizing proteomics, genomics and nanotechnology based diagnostics to aid in the detection as well as monitoring of many diseases including cancer.(Lee and Wong 2009; Malathi et al. 2014; Wong 2006) The analytes amount or concentration present in saliva is comparatively lower than the amounts presents in serum, which makes it perhaps an inappropriate candidate for diagnosis.(Streckfus and Bigler 2002) With advancement in sensitive diagnostic techniques, lower concentration of analytes in saliva is no longer a limitation.(Hu et al. 2008; Nagler et al. 2006; Nagler et al. 2002; Tan et al. 2008) Many researchers have been used saliva to detect OC by using cancer biomarkers including mi-RNA, IL-6 and IL-8.(Brailo et al. 2006; Li and Yang 2011; Malhotra et al. 2010; Ziober et al. 2008) Saliva has been also used to examine a range of drug levels, including cocaine, alcohol and marijuana.(Haeckel and Hanecke 1996) Saliva meets the requirements for noninvasive, inexpensive, and easy-to-use diagnostic methods. Saliva as diagnostic tool provide many advantages over serum, some of including noninvasive or pain free collection, low cost processing for analysis, easy handling and shipping.(Giannobile et al. 2009) The pain free collection of saliva reduces the discomfort and anxiety of patients. Blood processing requires anticoagulant agents when it is collected from the patients but saliva does not need any such agents for handling and processing.

The proteomic study of saliva has revealed many biomarkers related to the OC progression, which makes it a useful candidate with tremendous potential for OC monitoring and diagnosis.(Bahar et al. 2007; Nagler et al. 2006; Nagler et al. 2002; Wong 2006) A complete description about the OC biomarkers has been previously given by many authors, including anti-oncogenes (p53, p16), growth factors (EGF, IGF and VEGF), cytokeratins (CK13, CK16), epithelial tumour factors (CYFRA-21-1) and microRNA.(De Jong et al. 2010; Jou et al. 2010; Rajkumar et al. 2015; Warnakulasuriya et al. 2000; Zimmermann and Wong 2008) A list of OC biomarkers present in saliva has been summarised in **Table 1.** With

advancement of diagnostic technologies it can be possible to detect femto molar (fM) levels of cancer biomarkers in saliva.(Tan et al. 2008; Wang et al. 2013a) More recently use of saliva for detection of OC biomarkers emerged as novel and noninvasive approach.(Giannobile et al. 2009)

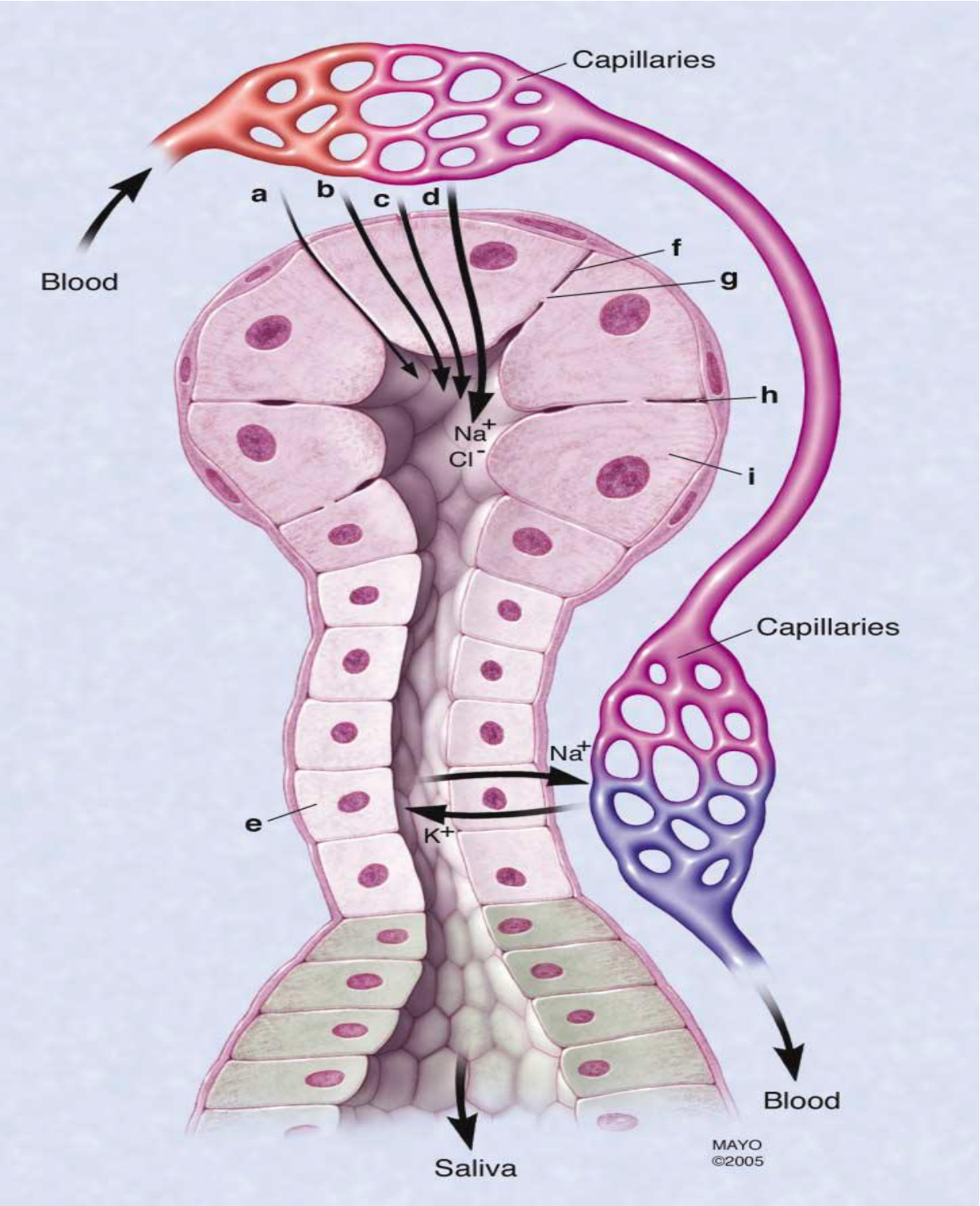


**Fig 1.** Mechanisms of transport of proteins and ions from serum into salivary gland ducts. **a**: active transport of selected compounds. **b**: passive diffusion of lipid soluble compounds. **c:** simple filtration of selected compounds. **d:** acinar cells actively pump sodium ions (Na+) into the duct, followed by water. **e:** duct cells pump Na+ back into blood, producing hypotonic saliva. **f:** cell membrane. **g:** pore of cell membrane. **h:** intracellular space. **i:** acinar cell. Cl−: chlorine ion. K+: potassium ion.(Haeckel and Hanecke 1996)

**Table 1. -** Biomarkers for OC detection present in saliva**:-**

| **Biomarkers** | **Reference** |
|---|---|
| IL-1 , IL-6, IL-8, TNF-α | (Rhodus et al. 2006) |
| CycD1 , Ki67, LDH, MMP-9, OGG1 , Maspin | (Shpitzer et al. 2009) |
| Telomerase | (Zhong et al. 2005) |
| p53 , Autoantibodies | (Warnakulasuriya et al. 2000) |
| Reactive nitrogen species | (Bahar et al. 2007) |
| HPV | (Zhao et al. 2005) |
| M2BP, MRP1 4, CD59, Profilin 1 Catalase | (Hu et al. 2008) |
| Transferrin | (Jou et al. 2010) |
| Salivary mRNA | (Zimmermann and Wong 2008) |
| 8- OHdG(oxidized DNA) | (Bahar et al. 2007) |
| ET-1 | (Pickering et al. 2007) |
| HNP-1 | (Mizukawa et al. 1997) |
| Salivary surviving | (Santarelli et al. 2013) |
| CYFRA-21-1 | (Lai et al. 1999; Nagler et al. 1999; Rajkumar et al. 2015) |

CYFRA-21-1 is a soluble fragment of cytokeratin 19, which is a component of cytoskeletal protein with a molecular weight of 40kDa.(Stieber et al. 1993) It is assumed that CYFRA-21-1 released in body fluid due to the cell death so the level of CYFRA-21-1 in body fluid correlates very well with the necrosis in the tumour.(Lai et al. 1999; Nagler et al. 1999)

A study evaluated salivary CYFRA-21-1 levels in OSCC using ELISA kits and compared with normal and found significantly increased levels in OSCC group. The study also found that the pre-operative saliva CYFRA-21-1 levels were significantly higher in patients suffering from tumor recurrence than in patients without recurrence.(Nagler et al. 1999; Rajkumar et al. 2015) The study highlights the usefulness of CYFRA-21-1 for tumor detection and predicting recurrence. It has been postulated that increased CYFRA-21-1 could be due to increased CK19 expression in tissues.(Lai et al. 1999)

## 3.4.2. Immobilization Matrices

A matrix can be utilized for immobilization or integration of desired biomolecules at a transducer surface and efficiently maintain the functionality of the biomolecules and at the same time provides accessibility towards the target analyte and an intimate contact with the transducer surface. Chemical properties of immobilizing matrix decide the immobilization method and the operational stability of a biosensor. For a preferred immobilizing matrix it should be resistant to a wide range of physiological pH, temperature, ionic strength and chemical composition.

Among the various immobilizing matrices, metal oxides receiving a great deal of attention owing to their exceptional optical and electronic properties. Their large surface area, high thermal and mechanical stability, abundant functional groups, biocompatibility and the

capability towards the direct electron transfer of proteins make them ideal candidate for the fabrication of a biosensor.(Kumar et al. 2015)

- **Nanostructured hafnium oxide for biosensing application**
  Hafnium is a tetravalent transition metal present in $IV^{th}$ group. Nanostructured hafnium oxide is an attractive inorganic metal oxide comprising of hafnium and oxygen elements. It can be prepared using soft chemistry i.e. one step low temperature hydrothermal process and sol-gel process.(Eliziário et al. 2009; Kidchob et al. 2007) It exhibits high surface to volume ratio, thermal stability, chemical inertness, nontoxicity, high-k and affinity for groups containing oxygen that make it an interesting material for biosensing application.(Fahrenkopf et al. 2012; Pan et al. 2010; Shim et al. 2013; Solanki et al. 2011) The isoelectric point of hafnium oxide is 7.0 that makes its surface neutral at physiological pH.(Fahrenkopf et al. 2012) Furthermore, oxygen moieties in $HfO_2$ can help to facilitate covalent attachment of linker molecules that can be useful for immobilization of biomolecules.(Fahrenkopf et al. 2012; Shim et al. 2013) In recent years, hafnium oxide attracts additional interest as possible candidate for biosensing application. Hafnium oxide has been widely used in field effective transistor (FET) based biosensing platform to detect biomolecules like mutated DNA, biomarkers etc. with improved sensitivity.(Chen et al. 2010) Lee et al. have proposed an invasive biosensor based on hafnium oxide for detection of human interleukin-10.(Lee et al. 2012) Jiwook Shim et al have shown the biosensing application of hafnium oxide nanopores. They demonstrated detection of dsDNA translocation through nanopore transistor under various applied bias levels and concluded that Hafnium oxide is a promising material for biosensing application .(Shim et al. 2013)

### 3.4.3. Transducer

A transducer is a device that converts a biological signal received from a biochemical reaction between a biological component and an analyte into an electronic signal. Transducer may be electrochemical, optical, thermal or piezoelectric depending upon the type of signal received. The electrochemical biosensors have recently aroused much interest due to their high signal-to-noise-ratio, simplicity, high sensitivity and fast response time.(Kumar et al. 2015; Wang 2006) Wang et al. reported an electrochemical and surface plasmon resonance aptasensor utilizing graphene for the detection of α-thrombin that exhibits high sensitivity and selectivity. A wide linear detection range of 0.03–200 nM was achieved with the detection limit of 0.03 nM.(Wang 2006) Malhotra et al. reported an ultrasensitive electrochemical immunosensor for oral cancer biomarker interleukin-6 (IL-6) detection using carbon nanotube forest electrodes and multilabel amplification. The highest sensitivity of 19.3 nA mL $pg^{-1}$ $cm^{-2}$ and detection limit (DL) of 0.5 pg $mL^{-1}$ (25 fM) in 10 μL of calf serum was reported. (Malhotra et al. 2012) Electrochemical biosensor offers many advantages over other transducers based biosensor, including wide linear response range, lower detection limit, high sensitivity, good stability, require lower sample amount etc.(Grieshaber, 2008 #549)

## 3.5. Biosensors for oral cancer detection

Biosensor development for sensitive and reliable measurement of biomarkers for cancer detection and prognosis is a significant challenge. Biosensor analyses of cancer biomarkers would reduce costs, required minimum sample amount ($\mu$L), ease of on-the-spot diagnosis, and lighten patient stress.(Arya and Bhansali 2011) Also biosensor measurements provide high accuracy and sensitivity, and require minimal technical expertise and system maintenance.

Available conventional methods for detection of cancer biomarkers have yet to satisfy all requirements for biosensor use.(Cady et al. 2009) Enzyme-linked immunosorbent assay (ELISA) is a gold standard commercially available method with lower detection limits (LDL) near 1 pg $mL^{-1}$ but is difficult to adapt to multiplexing.(Zangar et al. 2006) Bead-based or modified immunoassays using chemiluminescence, electrochemiluminescence, or fluorescence provide LDL approaching several pg $mL^{-1}$ but require high cost and high maintenance instruments for automated analyses.(Ambrosi et al. 2009) Newly available liquid chromatography−mass spectrometry (LC−MS) proteomics can provide multiple biomarker measurements at one spot approaching the sensitivity and detection limit, but still this method of measuring biomarkers is very expensive, labor intensive, and complex for routine diagnostics.(Deng et al. 2004) Emerging technologies for sensitive protein biomarker measurements, including biosensor based on electrochemical, optical, and nanotransistor detection.(Wang 2006; Ziober et al. 2008) Biosensors have many potential advantages over other conventional methods of cancer diagnosis and disease monitoring, especially increased response speed and flexibility. Rapid, real-time analysis of cancer biomarkers provide immediate required information to doctors and users that can be very helpful into the planning of patient care. Biosensor based analysis of cancer can improve the rate of earlier detection as well as monitoring of disease condition.(Wang 2006; Wei et al. 2009; Ziober et al. 2008)

Efforts have been made for the detection of OC utilizing biosensors platform. Yang et al. reported electrochemical biosensor for the detection of trace level of salivary IL-8 protein. However, in order to achieve the low level of detection streptavidin and HRP labeling of the receptor biomolecules were used which increased the complexity of detection.(Yang et al. 2005) In another approach, $CaCO_3$ nanoparticles based biosensor has been reported for IL-6 detection in serum sample. The major drawback of this method is that it is invasive and requires tagging of the receptor biomolecule, which make the whole process complicated.(Malhotra et al. 2012) Ivan H. El-Sayed et al. used surface plasmon resonance to detect EGFR into cell with the help of anti-EGFR conjugated gold nanoparticles. They reported the homogeneous and specific binding of conjugated nanoparticles to the surface of the cancer cells with an absorption maximum at 545 nm, while the binding of conjugated gold nanoparticles with noncancerous cells was nonspecific and random, with absorption maximum mostly around 552 nm. SPR absorption spectroscopy from anti-EGFR antibodies conjugated gold nanoparticles were found to distinguish between cancerous and noncancerous cells. The result of this study was effective but invasive nature and need that of highly expert personal for sample handling was the major drawbacks.(El-Sayed et al. 2005) Ruchika Mahrotra et al developed electrochemical immunosensor for human Inter Leukin-6 (IL-6 an Oral cancer Biomarker) detection. They used single wall carbon nanotube (SWCNT) forests with attached capture antibodies and enzyme label horseradish peroxidase

(HRP) to obtain very high sensitivity of 19.3 nA mL (pg IL-6)$^{-1}$ and detection limit (DL) of 0.5 pg mL$^{-1}$. The drawback of this biosensor pertains to the multienzyme labeling used to detect IL-6 concentration in calf serum (invasive sample collection) through electrochemical sandwich immunoassay protocol.(Malhotra et al. 2010)

Efforts have also been made to fabricate non-invasive biosensor for oral cancer detection ZongWeng Wang et al reported results of studies related to detection of micro-RNA (mi-RNA, an oral cancer biomarker) in saliva samples of Oral Cancer patients. They described a novel magnetic-controllable electrochemical biosensor for the ultra sensing of mi-RNA based on gold electrode. This electrode combined the merits of heated as well as magnetic electrode, has the advantage of strength and regulated direction of magnetic field. The advantage of gold electrode and magnetic beads- based enzymatic catalysis amplification, make the biosensor ultrasensitive to detect as low as 0.22 aM of mi-RNA. The sophisticated electrode fabrication made this biosensor costly and user unfriendly.(Wang et al. 2013b) To overcome all aforementioned drawbacks and problems, we have fabricated a highly efficient biofuntionalized nanostructured hafnium oxide ($HfO_2$) based biosensor for non-invasive Oral Cancer detection.

# Chapter-4

# Materials and methods

## 4.1. Chemicals and reagents

Hafnium dichloride oxide octahydrate (98+%) ($HfOCl_2.8H_2O$), cetyl trimethylammonium bromide (CTAB) ($C_{19}H_{42}BrN$) and 3-aminopropyl triethoxy silane (APTES) ($C_9H_{23}NO_3Si$) were purchased from AlfaAesar. 1-(3-(dimethylamino)-propyl)-3-ethylcarbodiimide hydrochloride (EDC) ($C_8H_{17}N_3$) of AR grade was purchased from Sigma Aldrich. Sodium hydroxide (NaOH) pellets, sodium monophosphte ($NaH_2PO_4$), sodium diphosphatedihydrate ($Na_2HPO_4.2H_2O$), N-hydroxysulfosuccinimide (NHS) ($C_4H_5NO_3$), sodium chloride (NaCl), potassium ferricyanide $\{K_3[Fe(CN)_6]\}$ and potassium ferrocyanide $\{K_4[Fe(CN)_6]3H_2O\}$ were purchased from Fisher Scientific. All the chemicals were of analytical grade and were used without any further purification. Phosphate buffer saline (PBS) solution of pH 7.0 was prepared using $Na_2HPO_4.2H_2O$ (0.05 mol L-1) and $NaH_2PO_4$ (0.05 mol L-1). Fresh PBS solution was prepared using Milli-Q water having resistivity of 18 MO cm and stored at 4 °C. Antigen CYFRA-21-1 and anti-CYFRA-21-1 were purchased from Ray Biotech, Inc., India. These biomolecules were further diluted using PBS buffer of pH 7.0. CYFRA-21-1 ELISA Kit was purchased from KinesisDX, USA.

## 4.2. Experimental

**4.2.1. Synthesis of hafnium oxide nanoparticles**: Low temperature hydrothermal process was used for the synthesis of hafnium oxide nanoparticles. We prepared solutions of 0.04 M of hafnium (IV) dichloride oxide octahydrate and 0.08 M sodium hydroxide in 70 mL of DI water. Next, 0.01 M CTAB solution was prepared in 10 mL of DI water. CTAB solution was added drop-wise in hafnium (IV) dichloride oxide octahydrate solution, after which it was kept for 2h at 25 °C with constant stirring. Further, sodium hydroxide was added drop-wise in above prepared solutions and kept for stirring for next 2h under similar conditions. Thus obtained solution contained in teflon was autoclaved and maintained at 170 °C for 17h. After cooling, the synthesized material was washed in DI water until the pH of the solution reached 7.0. Next, the whitish slurry was calcinated at 400 °C for 3h after which it was stored in a cool and dry place until further use. The mechanism of preparation of hafnium oxide nanoparticles is shown in **Scheme 3.**

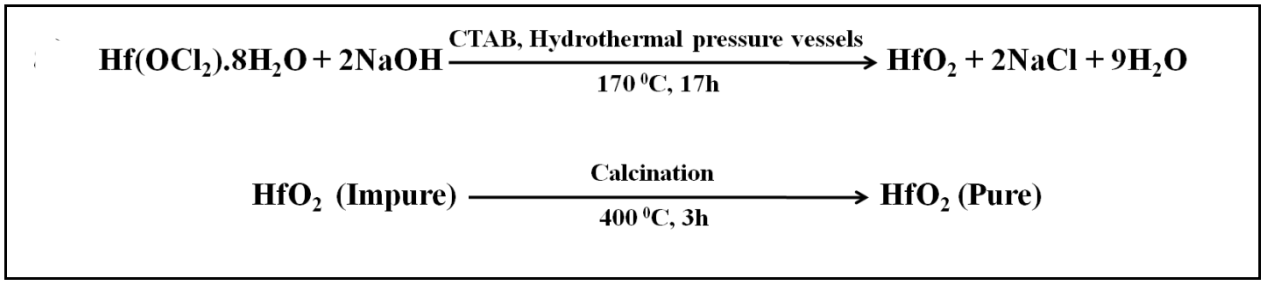


**Scheme 3.** Mechanism for synthesis of hafnium oxide nanoparticles.

**4.2.2. Functionalization of hafnium oxide nanoparticles and electrophoretically deposition on ITO electrode (APTES/$HfO_2$/ITO):** The obtained hafnium oxide nanoparticles are functionalized through a low temperature silanization process. The dispersed 200 mg of hafnium oxide nanoparticles in 50 mL of isopropanol are further added to 0.6g of 98% APTES drop-wise after which 20 mL of DI water is added and kept for stirring at 300 rpm for 48h at 50 °C. To remove unbounded APTES molecules, these nanoparticles were washed with DI water and stored in a dry place.

Indium tin oxide coated glass (ITO) electrode is used as a substrate for fabrication of biosensing platform. 1 mg mL-1 of these functionalized hafnium oxide nanoparticles are dispersed in acetonitrile. Electrophoretic deposition (EPD) technique (genetix, GX300C instrument) was used for deposition of functionalized nanoparticles. 22V was applied for 30s for EPD of APTES/$HfO_2$ onto the pre hydrolyzed ITO electrode.(Kumar et al. 2011) An optimized surface area of the APTES/$HfO_2$/ITO electrode was determined to be 0.25 $cm^2$. The prepared electrode was washed with DI water and dried at 25 °C.

**4.2.3. Fabrication of BSA/anti-CYFRA-21-1/APTES/$HfO_2$/ITO immunoelectrode:** 15 µL of anti-CYFRA-21-1 (50 µg mL-1) was mixed with 7.5 µL of 0.4 M EDC (activator) and 7.5 µL of 0.1 M NHS (coupling agent) for activation of -COOH groups of the antibody molecules. Further, this solution (30 µL) was uniformly spread by drop-casting method onto APTES/$HfO_2$/ITO electrode. The electrode was kept in a humid chamber at 25 °C for 3h followed by washing with PBS to remove any unbound antibody molecules. -COOH group of anti-CYFRA-21-1 was thus covalently bound with -$NH_2$ terminal of APTES via strong amide bond (OC-NH). Further, bovine serum albumin (BSA = 1 mg dL-1) (20 µL) was used for blocking the nonspecific active sites of the electrode. After washing of fabricated BSA/anti-CYFRA-21-1/APTES/$HfO_2$/ITO immunoelectrode with PBS to remove unbound BSA, the immunoelectrode was stored at 4 °C under dark conditions until further use. Scheme 1 (b) shows a stepwise fabrication process of the BSA/anti-CYFRA-21-1/APTES/HfO2/ITO immunosensor. Collection and processing of saliva samples: Unstimulated whole saliva was collected from ten patients diagnosed for the oral cancer. DI water (5 mL) was used for rinsing of mouth and expectorated into sterilized tube, kept in ice condition. The collected saliva was centrifuged at 2800 rcf at room temperature for 30 minutes after which the supernatant was collected in sterilized tube and stored at -20 °C. (Rajkumar et al. 2015) The saliva samples of oral cancer patient were collected from Rajiv Gandhi Cancer Institute and Research Centre, Delhi (India). All saliva samples were collected under a protocol approved by Rajiv Gandhi Cancer Institute and Research Center Review Board and all the patients were provided with written informed consent.

**4.2.4. Collection and processing of saliva samples:** Unstimulated whole saliva was collected from ten patients diagnosed for the oral cancer. DI water (5 mL) was used for rinsing of mouth and expectorated into sterilized tube, kept in ice condition. The collected saliva was centrifuged at 2800 rcf at room temperature for 30 minutes after which the supernatant was collected in sterilized tube and stored at -20 ˚C.(Rajkumar et al. 2015) The saliva samples of oral cancer patient were collected from Rajiv Gandhi Cancer Institute and Research Centre, Delhi (India). All saliva samples were collected under a protocol approved by Rajiv Gandhi Cancer Institute

and Research Center Review Board and all the patients provided written informed consent.

## 4.3. Characterization

Crystallinity and phase information of synthesized product was obtained by using monochromatic X-ray diffraction (XRD) pattern [Bruker D-8 Advance] with Cu-Ka radiation (**λ**=1.5406 Å). Morphological observations and particle size were carried out using transmission electron microscopy at an accelerating voltage of 200 kV (Tecnai G2 30 U-twin, Tecnai 300 kV ultratwin microscope). The topography of APTES/$HfO_2$/ITO, anti-CYFRA-21-1/APTES/$HfO_2$/ITO and BSA/anti-CYFRA-21-1/APTES/$HfO_2$/ITO electrodes were investigated using atomic force microscopy (AFM) on a Park Xe-100 AFM system. X-ray photoelectron spectroscopy (XPS) has been performed using Nova, Kratos Analytical Ltd., Manchester, UK. Next, functional groups and bonds present in APTES/$HfO_2$/ITO and anti-CYFRA-21-1/APTES/$HfO_2$/ITO were investigated through Fourier transform infrared spectroscopy (FT-IR) [PerkinElmer, Spectrum BX II]. The Autolab Potentiostat (Netherlands) was used for the electrochemical response studies by using a three-electrode system. The fabricated electrode acted as the working electrode, Ag/AgCl as the reference electrode and platinum (Pt) as the counter electrode.

### 4.3.1. X-ray diffraction (XRD) technique

Max von Laue, in 1912, discovered that crystalline substances act as three- dimensional diffraction gratings for X-ray wavelengths similar to the spacing of planes in a crystal lattice. X-ray diffraction is an effective tool in studying the nature of crystalline substances. It is based on constructive interference of monochromatic X-rays and a crystalline sample. These X-rays are generated by a cathode ray tube, filtered to produce monochromatic radiation, collimated to concentrate, and directed toward the sample. The interaction of the incident rays with the sample produces constructive interference (and a diffracted ray) when conditions satisfy Bragg's Law (**Eq. 1**)

$$2d\ Sin\ \theta = n\ \lambda \quad \ldots\ldots\ldots\ldots \text{Eq. 1}$$

where $\lambda$ is the wavelength of electromagnetic radiation, $\theta$ is the diffraction angle and $d$ is the lattice spacing in a crystalline sample. These diffracted X-rays are then detected, processed and counted. By scanning the sample through a range of 2θ angles, all possible diffraction directions of the lattice is attained due to the random orientation of the powdered material. This technique is used to characterize the crystallographic structure, crystallite size (grain size) and preferred orientation in polycrystalline or powder solid samples.

XRD can be applied to characterize the heterogeneous solid mixture to determine relative abundance of a crystalline compound. It is also useful in providing information on the structure of unknown sample when coupled with lattice refinement technique such as relative refinement. XRD patterns are recorded on X-ray diffractometer, wherein the peak broadening data are obtained by measuring the average of peak broadening in the five

strongest diffraction peaks. The mean size of the nanoparticles is determined from the peak broadening in the X-ray diffraction pattern by using Debye– Scherrer equation (Eq. 2) .

$$D = \frac{0.9\lambda}{\beta Cos\theta} \ldots\ldots\ldots\ldots\ldots\ldots \text{Eq. 2}$$

where $D$ is the average crystallite size (Å), $\lambda$ is wavelength of X-rays (Cu Kα: $\lambda$ = 1.5418 Å), $\theta$ is the Bragg diffraction angle, and $\beta$ is the full width at half maximum (FWHM) (in radians). The sample under study can be of either a thin layer of crystal or in powder form. Since the power of a diffracted beam is dependent on quantity of corresponding crystalline substance; it is also possible to carry out quantitative determinations using this technique.

### 4.3.2. Transmission Electron Microscopy (TEM)

It is a microscopic technique in which a beam of electron passes through an ultra-thin specimen for the interaction with sample. Electrons are accelerated with 100keV-1 MeV to project onto a specimen of less than 200 nm through the help of condenser lens system. The interaction of electron beam and sample results in image formation which is further focused and magnified on imaging device or detected by the CCD camera. TEM provides high resolution images (ranging from 50 to $10^6$) than the light microscope.

A TEM is constituted of: (1) two or three condenser lenses to focus the electron beam on the sample, (2) an objective lens to form the diffraction in the back focal plane and the image of the sample in the image plane, (3) some intermediate lenses to magnify the image or the diffraction pattern on the screen. TEM is commonly operated in Bright Field (BF) imaging mode. In BF mode the contrast formed directly by absorption and occlusion of electrons in the sample. Sample regions with thickness or higher atomic number will appear dark and the region with no sample will appear bright. Other then structural characterization of nanomaterials (NMs) TEM can also be used to determine NM's melting point. The melting point of NMs determine by the electron diffraction disappearance which results due to the heat up of NMs with electron beam. Beside this TEM also can be used to study the electrical and mechanical properties of nanotubes and nanowires.

### 4.3.3. Atomic Force Microscopy (AFM)

The atomic force microscopy (AFM), also known as scanning force microscopy (SFM) is a very high-resolution type of scanning probe microscopy (SPM), which can achieve resolution of fractions of a nanometer. It works in the same way as our fingers that touch and probe the environment when we cannot see it. By using a finger to "visualize" an object, human brain deduces its topography while touching it. Atomic Force Microscope was developed to overcome a basic drawback with Scanning Tunneling Microscopy (STM) - that it can only image conducting or semiconducting surfaces. The AFM consists of a microscale cantilever with a sharp tip (probe) at its end that is used to scan the specimen surface. When the tip is brought into proximity of a sample surface, forces between the tip and the sample lead to a deflection of the cantilever. As AFM relies on the forces between the tip and the sample, knowing these forces is important for

proper imaging.

The force is calculated by measuring the deflection of the lever, and knowing the stiffness of the cantilever using Hooke's law. Forces that act between the sample and the tip will not only cause a change in the oscillation amplitude, but also change in the resonant frequency and phase of the cantilever.

### 4.3.4. Fourier Transform Infrared (FT-IR) Spectroscopy

FT-IR is an analytical technique that can be used for structural characterization of organic materials. It is a chemically specific analysis technique that can be used to identify chemical compounds and substituent groups. When a quanta of infra red light interact with the molecule, it may absorb energy and vibrate faster. This phenomenon is the basis of FT-IR spectroscopy. Infra red absorption only occurs when infrared radiation interacts with a molecule undergoing a change in dipole, and when the incoming photon has sufficient energy for the transition to the next allowed vibrational energy states. These infrared absorption bands identify specific molecular components and structures. In the FT-IR spectra, the appearance or non-appearance of certain vibrational frequencies gives valuable information about the structure of a particular molecule. Each functional group has specific range of vibrational frequencies and is very sensitive to the chemical environment, thus providing valuable information regarding the presence of certain functional groups in the specific sample for their further characterization. FTIR spectrophotometer has a spectrum in the range of 400-4000 $cm^{-1}$.

### 4.3.5. X-ray Photoelectron Spectroscopy (XPS)

X-ray photoelectron spectroscopy (XPS) is an important and widely used surface chemical analysis method in a many fields of study including physics and chemistry. The phenomenon is based on the photoelectric effect outlined by Einstein in 1905 where the electrons are ejected from an atomic energy level by an X-ray photon (*Al-Kα* or Mg-Kα), and its energy is analyzed by the spectrometer. Only those electrons which are escaped from the sample into the vacuum of the instrument and reached to the detector are detected by the XPS. For each and every element, there is a characteristic binding energy associated with each core atomic orbital i.e. each element gives rise to a characteristic set of peaks in the photoelectron spectrum at kinetic energies determined by the photon energy and the respective binding energies. The presence of peaks at particular energies, therefore, indicates the presence of a specific element in the sample under study. Furthermore, intensity of the peaks is related to the concentration of element within the sampled region. Thus, the technique provides a quantitative analysis of surface composition and is sometimes known by the alternative acronym, ESCA (Electron Spectroscopy for Chemical Analysis). XPS is not sensitive to hydrogen and helium, but can detect all other elements. The analysis and detection of photoelectrons in XPS requires the sample to be placed in a high-vacuum chamber. Since the photoelectron energy depends on X-ray energy, the excitation source must be monochromatic.

### 4.3.6. Electrochemical Techniques

Electrochemical techniques relate the changes of an electrical signal to an electrochemical reaction at an electrode surface, usually as a result of an imposed potential or current. In a solution, the equilibrium concentrations of the reduced and oxidized forms of a redox couple are linked to the potential (E) via the **Nernst's Equation (Eq. 3)**.

$$E = E_o + \frac{RT}{nF} \ln \frac{Coxi}{Cred} \quad \text{.....Eq.3}$$

where, $E_O$ is equilibrium potential, ~~$F$~~ is F~~arad~~ay's constant, $T$ is absolute temperature, $C_{oxi}$ and $C_{red}$ are concentrations of oxidation and reduction centers. If the potential $E$ is applied to the working electrode with respect to the reference electrode e.g. via Potentiostat, the redox couples present at the electrode respond to this change and adjust their concentration ratios according to Eq. 3.

Cyclic voltammetry is a versatile potentiodynamic electroanalytical technique that is employed to study the electrochemical properties of electroactive species. To obtain a cyclic voltammogram, the voltage is varied in the solution and change in current is measured with respect to the change in voltage. It is an electrolytic method that uses microelectrodes and an unstirred solution so that the measured current is limited by analyte diffusion at an electrode surface.

In a CV experiment, current response over a range of potentials (a potential window) is measured, starting at an initial value and varying the potential in a linear manner up to a pre-defined limiting value. The current increases as the voltage reaches the oxidation potential of the analyte, after which it falls off as the concentration of the analyte is depleted close to the electrode surface. At this potential (often referred to as a switching potential), the direction of the potential scan is reversed, and the same potential window is scanned in the opposite direction (hence the term cyclic). As the applied potential is reversed, it will reach a potential where the reduction of product formed during forward scan starts producing a current of reverse polarity from the forward scan. This reduction peak will usually have a similar shape as that of an oxidation peak in other direction. Non-symmetric peaks are attributed to a quasi-reversible reaction. If the process is completely irreversible, the anodic peak does not appear in the measurable potential region. As a result, information about the redox potential and nature of electrochemical reactions is obtained. The important parameters that can be derived from CV are magnitude of peak current ($Ip$), peak potential ($Ep$), number of electrons transferred per reactant molecule ($n$), rate constant, diffusion coefficient ($D$) and electrochemical reversibility. The peak current ($Ip$) for a reversible system is described by the **Randles-Sevcik equation (Eq. 4)**

$$I_P = 2.69 \times 10^5 A D^{1/2} n^{3/2} \gamma^{1/2} C \quad \text{..... Eq. 4}$$

# Chapter-5

# Results and discussion

## 5.1. Structural and morphological studies:

The results of X-ray diffraction (XRD) pattern of $HfO_2$ nanoparticles are shown in the **Figure (2a)**. The diffraction peaks corresponding to (011), (1-11), (111), (020), (201), (-202), (022), (310) and (-222) planes indicate the formation of a single monoclinic phase (JCPDS 34-0104). The TEM image shown in **Figure 2b** indicates agglomeration and polydispersive nature of $HfO_2$ nanoparticles due to which a rectangular shape structure is formed. This agglomeration is due to the Brownian motion of the suspended dispersed molecules in solution.(Eliziário et al. 2009; Lee et al. 2006) As discussed in literature, two nanoparticles having the same crystallographic orientation can undergo adhesion process with highest probability. (Eliziário et al. 2009; Lee et al. 2006) According to this phenomenon, nanoparticles remain attached due to *Vanderwaals* forces and coalescence occurs. (Eliziário et al. 2009; Lee et al. 2006) The HRTEM image of a typical oval shaped $HfO_2$ nanoparticle indicates an average particle size of 14 nm (**Figure 2c**). **Figure 2d** shows lattice fringes of $HfO_2$ nanoparticles. The average lattice spacing is 1.79 Å which corresponds to (022) of the crystallographic plane.

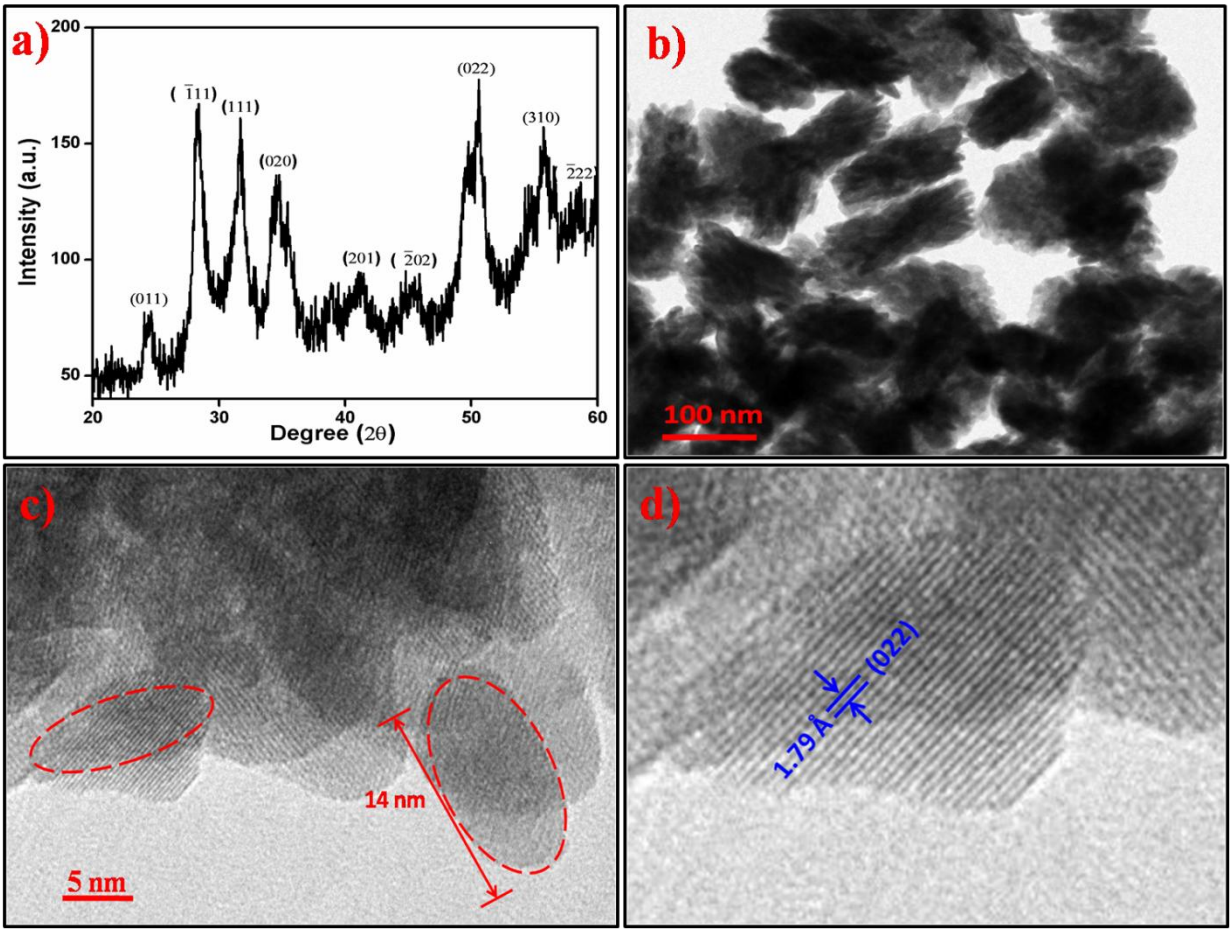


**Figure 2. (a)** XRD pattern **(b)** TEM image **(c-d)** HR-TEM image of $HfO_2$ nanoparticles.

The surface morphology (2-D and 3-D view) of i) APTES/$HfO_2$/ITO ii) anti-CYFRA-21-1/APTES/$HfO_2$/ITO and iii) BSA/anti-CYFRA-21-1/APTES/$HfO_2$/ITO electrodes have been investigated using atomic force microscopy (AFM) in the tapping mode and is shown in **Figure 3 (a-f)**. The AFM image of APTES/$HfO_2$/ITO shows that functionalized $HfO_2$ nanoparticles are uniformly distributed onto the ITO surface resulting in the nanoporous structure with an average roughness of ~4.66 nm. However, after the immobilization of anti-CYFRA-21-1 on APTES/$HfO_2$/ITO electrode the average roughness increases to ~7.07 nm. Here a regular globular morphology is observed which reveals high loading of the antibody molecules onto APTES/$HfO_2$ surface via covalent interactions. Further, after BSA treatment the BSA/anti-CYFRA-21-1/APTES/$HfO_2$/ITO electrode reveals an average roughness of ~5.54 nm. The decrease in roughness of the BSA/anti-CYFRA-21-1/APTES/$HfO_2$/ITO immunoelectrode is due to the presence of BSA molecules which block the nonspecific binding sites of the immunoelectrode surface.

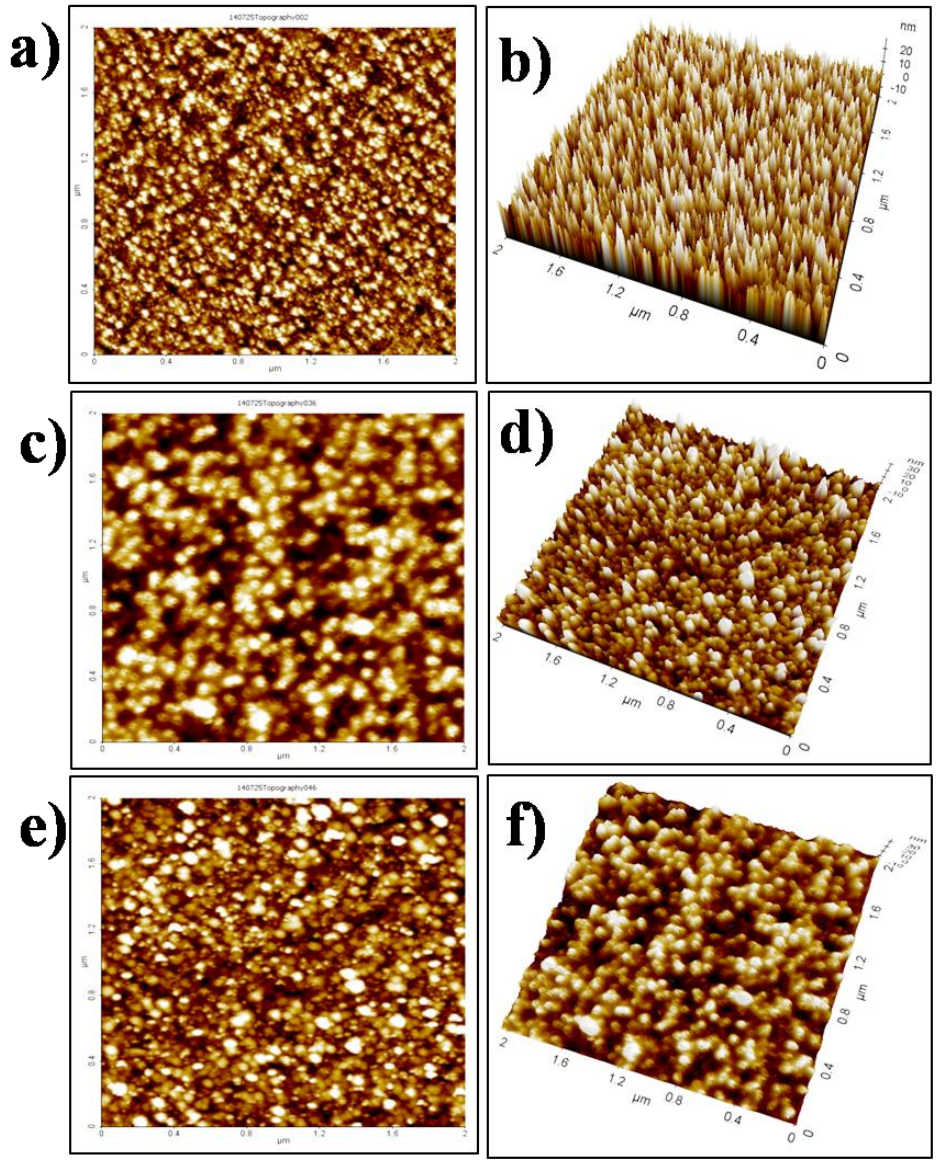


**Figure 3.** 2D and 3D AFM images of APTES/$HfO_2$/ITO **(a-b),** anti-CYFRA-21-1/APTES/$HfO_2$/ITO **(c-d)** and BSA/anti-CYFRA-21-1/APTES/$HfO_2$/ITO **(e-f)**.

## 5.2. X-ray photoelectron spectroscopy (XPS) studies

Nanostructured hafnium oxide functionalized with 3-aminopropyltriethoxy silane (APTES) has been investigated by XPS study. **Figure 4** shows wide scan XPS of (a) $HfO_2$ and (b) APTES/$HfO_2$. In both spectra, the characteristic peaks observed at 16.0, 212.5, 223.2 and 530.1 eV are assigned to Hf $4f^{7/2}$, Hf $4d^{5/2}$, Hf $4d^{3/2}$ and O1s respectively.(Ali et al. 2013; Crist 2000) In the spectrum (b), additional peaks are observed at 101.6, 285.1 and 399.4 eV due to the presence of Si, C 1s and N 1s respectively confirming functionalization of $HfO_2$ nanoparticles with APTES.(Ali et al. 2013; Crist 2000) Further, XPS spectra of hafnium 4f, Oxygen 1s and nitrogen 1s regions of $HfO_2$ and APTES/$HfO_2$ were deconvoluted into characteristic binding energy peaks using Shirley-type baseline and Lorentzian-Doniac-Sunsic curves, with a Gaussian profile as shown in **Figure 4 (c-g)**. In **Figure 4 (c and d)**, the peak observed at 16.0 eV is hafnium (4f) and the peak seen at 17.5 eV indicates the presence of bond between hafnium and oxygen molecules.(Crist 2000) **Figure 4 (e and f)** represents O 1s spectra of $HfO_2$ and APTES/$HfO_2$. Binding energy peak found near 529.5 indicates $O^{2-}$ states of $HfO_2$ while the peak seen at 531 eV is perhaps due to other chemical states of oxygen (C-O, C=O) [**Figure 4 (d and f)**].(Crist 2000) **Figure 4 (g)** shows the N 1s spectra where a typical binding energy peak found at 398.5 eV is due to the N 1s electrons whereas the peak seen at 399.4 eV is attributed to the nitrogen present in free amino groups of APTES molecules.(Ali et al. 2013; Gorschinski et al. 2009) The observed results indicate functionalization of hafnium oxide nanoparticles with APTES molecules that can be used for covalent immobilization of -COOH containing biomolecules.

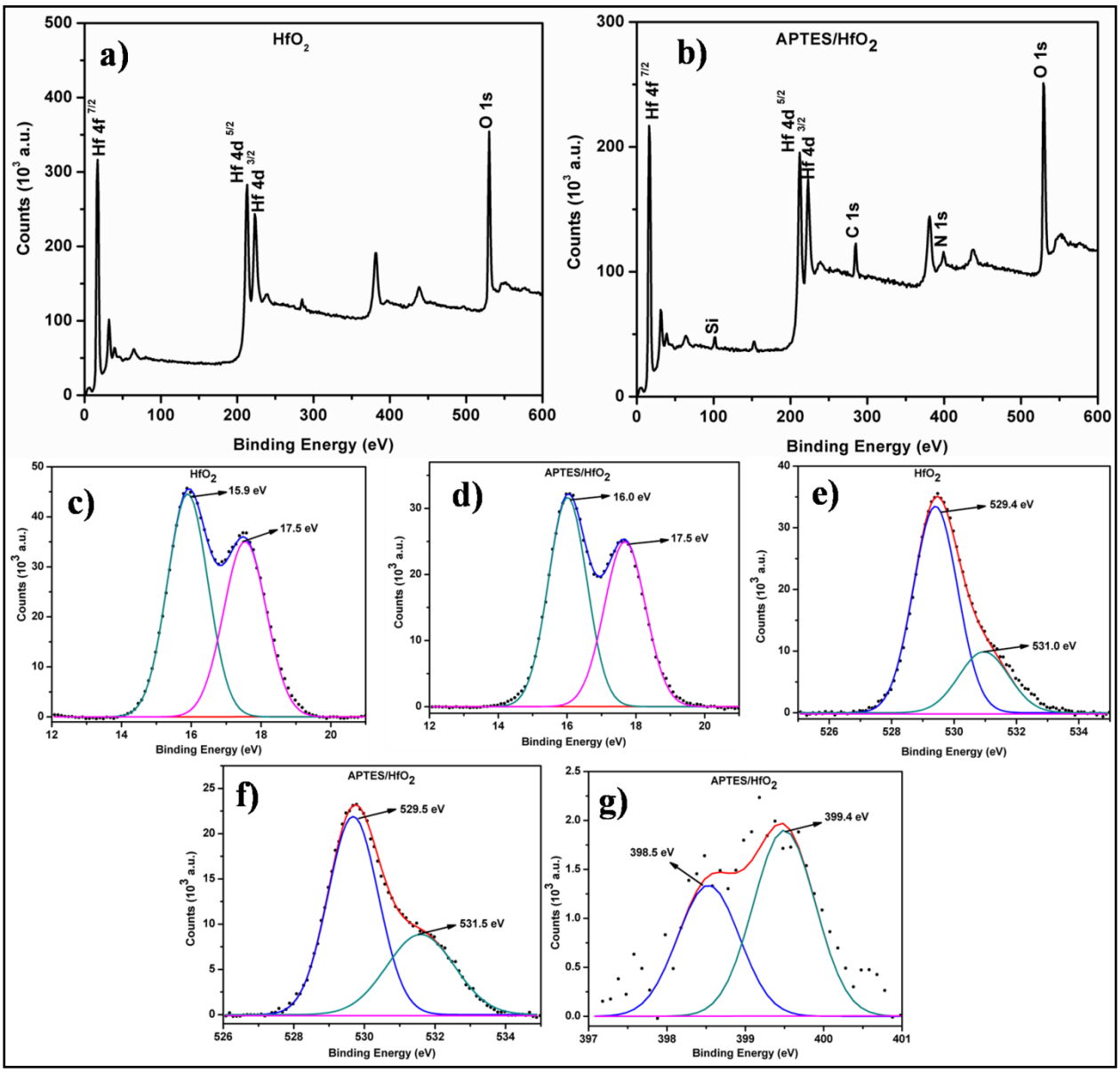


**Figure 4.** Wide-scan X-ray photoelectron spectra (XPS) of **(a)** $HfO_2$ and **(b)** APTES/$HfO_2$. XPS spectra of **(c)** Hf $4f^{7/2}$ of $HfO_2$ **(d)** Hf $4f^{7/2}$ of APTES/$HfO_2$ **(e)** O 1s of $HfO_2$ **(f)** O 1s of APTES/$HfO_2$ and **(g)** N 1s of APTES/$HfO_2$.

## 5.3. Fourier transformed infra-red spectroscopic (FT-IR) studies

To confirm the APTES functionalization of $HfO_2$ nanoparticles and the immobilization of anti-CYFRA-21-1 on APTES/$HfO_2$/ITO electrode, FT-IR studies have been conducted. FT-IR spectra of the APTES/$HfO_2$/ITO and anti-CYFRA-21-1/APTES/$HfO_2$/ITO electrodes are shown in **Figure 5 (a and b)**, respectively. Both the spectra show peak at 495 $cm^{-1}$ indicating presence of Hf=O bond.(Kidchob et al. 2007) The FT-IR spectra of APTES/$HfO_2$/ITO electrode shows intense peak at 1561 $cm^{-1}$ corresponding to -$NH_2$ group on the free surface. The peak seen at 2567 $cm^{-1}$ is due to the presence of C-H bond present in the APTES molecules with $sp^3$ hybridization, a broad peak is present between 2900 to 3400 $cm^{-1}$ due to immersion of N-H stretching vibration with -OH stretching of water molecules.(Ali et al. 2013) Further, FT-IR spectra of the anti-CYFRA-21-1/APTES/$HfO_2$/ITO electrode exhibits a prominent peaks found at 1600 and 1746 $cm^{-1}$ that are due to the presence of C-N stretching

of amide bond II indicating immobilization of anti-CYFRA-21-1 on the APTES/$HfO_2$/ITO electrode.(Ali et al. 2013)

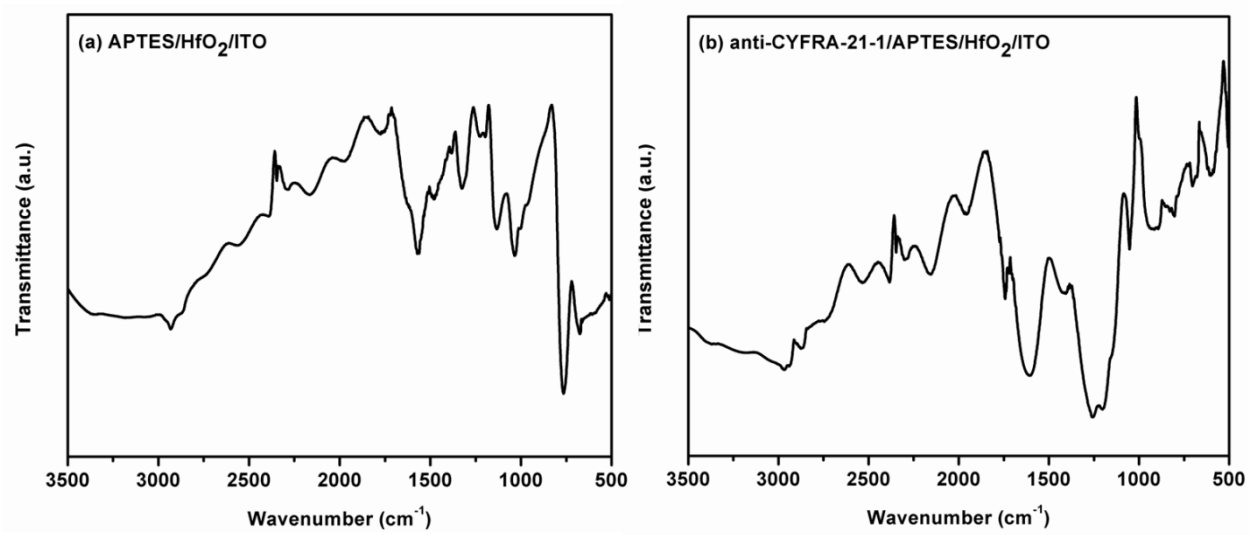


**Figure 5.** FTIR spectra of **(a)** APTES/$HfO_2$/ITO and **(b)** anti-CYFRA-21-1/APTES/$HfO_2$/ITO electrodes.

## 5.4. Electrochemical studies

The pH studies have been conducted on the fabricated immunoelectrode (BSA/anti-CYFRA-21-1/APTES/$HfO_2$/ITO) using cyclic voltammetry (CV) in PBS (50 mM, 0.9% NaCl) buffer at different pH 6.0, 6.5, 7.0, 7.4, 8.0, with $[Fe(CN)_6]^{3-/4-}$ (5mM) at scan rate of 50 mV/s in the potential range -0.8 to 0.8 V. It has been found that this electrode exhibits maximum current at pH 7.0 (**Figure 6.**). This may be due to the fact that biological molecules (such as amino acid, enzyme, antigen, antibody etc.) are present in natural form with high activity at neutral pH. However, in acidic or basic medium antibodies get denatured due to the effect of $H^+$ or $OH^-$ ions on the amino acid sequence of antibody.(Kumar et al. 2011; Liu and Lin 2005) Therefore, further electrochemical measurements have been performed in the buffer with pH 7.0.

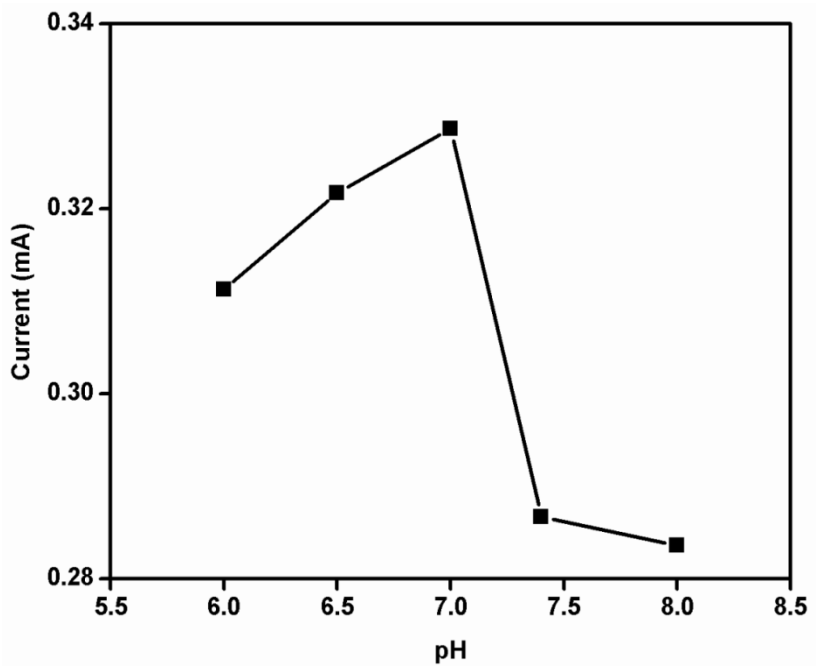


**Figure 6.** pH response of BSA/anti-CYFRA-21-1/APTES/$HfO_2$/ITO

The CV of ITO, APTES/$HfO_2$/ITO, anti-CYFRA-21-1/APTES/$HfO_2$/ITO and BSA/anti-CYFRA-21-1/APTES/$HfO_2$/ITO electrodes have been recorded (**Figure 7.**). The anodic peak current of ITO electrode ($I_{pa}$= 0.402 mA) is found to decrease in case of the APTES/$HfO_2$/ITO electrode ($I_{pa}$= 0.181 mA). On the other hand peak current of the anti-CYFRA-21-1/APTES/$HfO_2$/ITO immunoelectrode ($I_{pa}$= 0.342 mA) increases with respect to the APTES/$HfO_2$/ITO electrode. It indicates that the nanostructured APTES/$HfO_2$/ITO electrode provides a favorable microenvironment and spatial orientation for the immobilized antibody molecules leading to higher current.(Fahrenkopf et al. 2009; Lee et al. 2012) The peak current of the BSA/anti-CYFRA-21-1/APTES/$HfO_2$/ITO immunoelectrode ($I_{pa}$= 0.338 mA) decreases. This is because BSA molecules block most of the non-specific active sites present on the immunoelectrode surface resulting in hindered electron transfer between the solution and electrode.

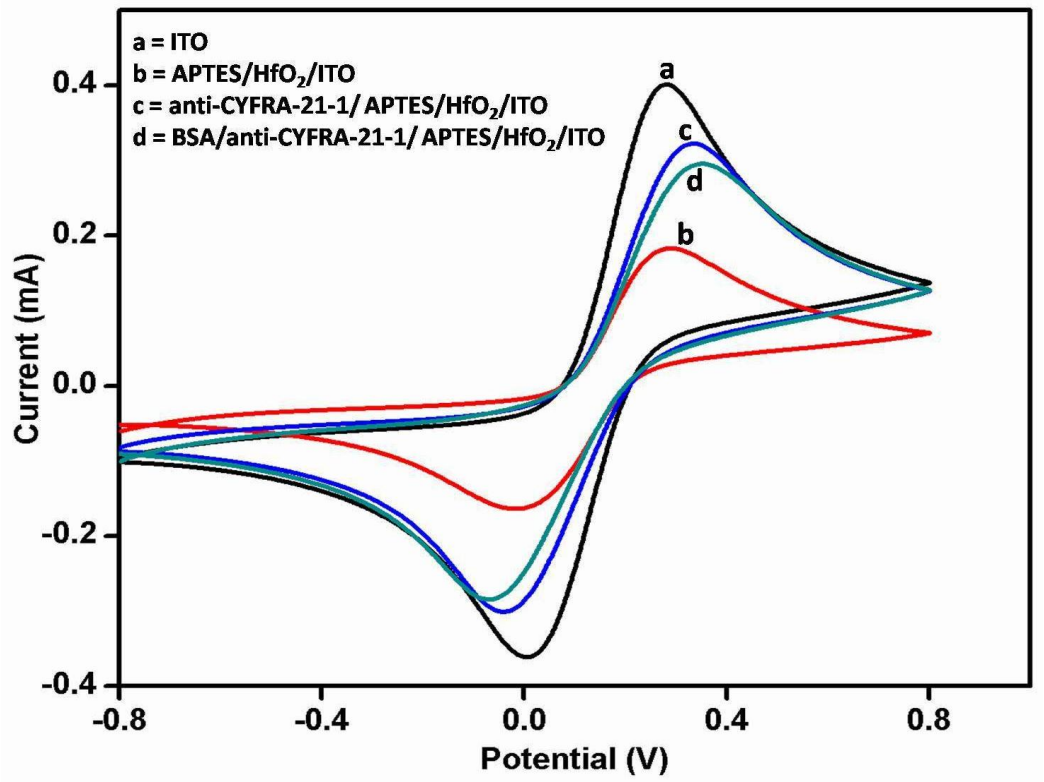


**Figure 7.** Cyclic voltammetry response studies of (a) ITO (b) APTES/$HfO_2$/ITO (c) anti-CYFRA-21-1/APTES/$HfO_2$/ITO and d) BSA/anti-CYFRA-21-1/APTES/$HfO_2$/ITO electrodes.

The scan rate response studies have been conducted on fabricated APTES/$HfO_2$/ITO electrode and BSA/anti-CYFRA-21-1/APTES/$HfO_2$/ITO immunoelectrode in the range of 40-150 mV/s as shown in **Figure 8 and 9,** respectively. The peak-to-peak separation of both the electrodes increases and shifts toward the higher potential side with increasing scan rate leading to diffusion controlled (quasi-reversible) process.(Kumar et al. 2011; Vasudev et al. 2013) The **Inset A of Figure 8 and 9** shows plot between the anodic ($I_{pa}$) and cathodic ($I_{pc}$) peak current versus square root of scan rate. The linear curve fitting gives the following equations:

$$I_{pa\ (APTES/HfO2/ITO)} = [18.2\ \mu A(s/mV) \times (\text{scan rate}[mV/s])^{1/2}] + 48.97\ \mu A,$$

$R^2 = 0.999$ …….(i)

$I_{pc\ (APTES/HfO2/ITO)} = -[17.52\ \mu A(s/mV) \times (\text{scan rate}[mV/s])^{1/2}] - 39.15\ \mu A$,
$R^2 = 0.999$ ..…….(ii)

$I_{pa\ (BSA/anti\text{-}CYFRA\text{-}21\text{-}1/APTES/HfO2/ITO)} = [44.17\ \mu A(s/mV) \times (\text{scan rate}[mV/s])^{1/2}] + 21.71\ \mu A$,
$R^2 = 0.999$ …….(iii)

$I_{pc\ (BSA/anti\text{-}CYFRA\text{-}21\text{-}1/APTES/HfO2/ITO)} = -[35.10\ \mu A(s/mV) \times (\text{scan rate}[mV/s])^{1/2}] - 84.10\ \mu A$,
$R^2 = 0.998$ …….(iv)

**Inset B in Figure 8. and 9.**show the plot between the potential peak shift ($\Delta V = V_{pa} - V_{pc}$, $V_{pa}$ is anodic peak potential and $V_{pc}$ is cathodic peak potential) and square root of the scan rate obtained for APTES/$HfO_2$/ITO and BSA/anti-CYFRA-21-1/APTES/$HfO_2$/ITO electrode, respectively. The linear curve fitting gives the following equations:

$\Delta V_{APTES/HfO2/ITO} = [0.042\ V(s/mV) \times (\text{scan rate}[mV/s])^{1/2}] + 0.17\ V$,
$R^2 = 0.997$…..….(v)

$\Delta V_{BSA/anti\text{-}CYFRA\text{-}21\text{-}1/APTES/HO2/ITO} = [0.031\ V(s/mV) \times (\text{scan rate}[mV/s])^{1/2}] + 0.53V$,
$R^2 = 0.997$ …….(vi)

These linear relationships indicate that electrochemical reactions are diffusion controlled (quasi-reversible).(Vasudev et al. 2013) The diffusion coefficient (or diffusivity) of the redox species {$[Fe(CN)_6]^{3-/4-}$} has been estimated using Randles-Sevcik equation.

$$I_p = (2.69 \times 10^5)\, n^{3/2} A D^{1/2} C v^{1/2} \quad \text{…….……(vii)}$$

where $I_p$ is the peak current of the immunoelectrode, n is the number of electrons transferred (1), A is surface area of the electrode (0.25 $cm^2$), D is diffusion coefficient, C is the concentration of redox species ($5\times10^{-3}$ mol $cm^{-2}$) and v is the scan rate (50 mV $s^{-1}$). The diffusion coeffcient has been obtained as $2.12 \times 10^{-3}$ $cm^2$ $s^{-1}$. The surface concentration of BSA/anti-CYFRA-21-1/APTES/$HfO_2$/ITO immunoelectrode has been estimated through Brown-Anson model as given in equation viii:

$$I_p = n^2F^2\gamma A\upsilon(4RT)^{-1} \quad \text{……..……(viii)}$$

where $I_p$ represents the peak current, A is the surface area of the electrode, ν is the scan rate (V/s), γ is the surface concentration of the absorbed electro-active species, F is the Faraday constant (96485 C $mol^{-1}$), R is the gas constant (8.314 J $mol^{-1}$ $K^{-1}$) and T is room temperature (25 ˚C or 298 K). The surface concentration of BSA/anti-CYFRA-21-1/APTES/$HfO_2$/ITO is estimated as $2.87 \times 10^{-8}$ mol $cm^{-2}$.(Singh et al. 2013; Singh et al. 2012)

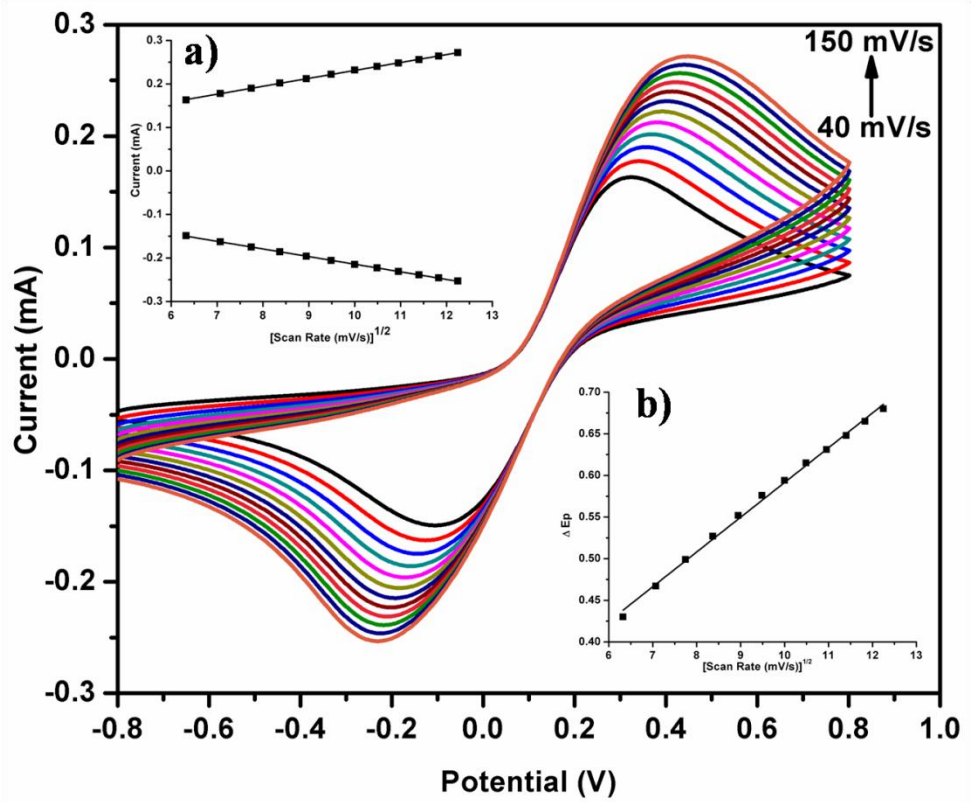


**Figure 8.** Cyclic voltammogram (CV) studies of APTES/$HfO_2$/ITO electrode as a function of scan rate (40-150 mV/s), Inset (a) magnitude of oxidation and reduction current generated as response of scan rate (mV/s), Inset (b) potential as function of scan rate.

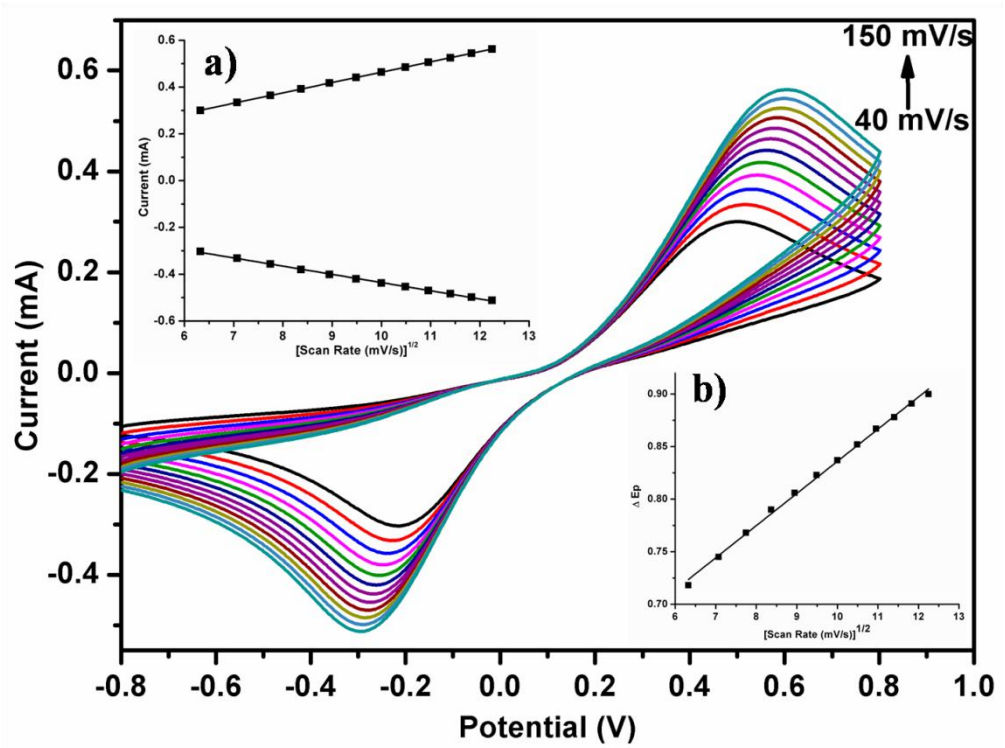


**Figure 9.** CV studies of BSA/anti-CYFRA-21-1/APTES/$HfO_2$/ITO immunoelectrode as a function of scan rate (40-150 mV/s), Inset (a) magnitude of oxidation and reduction current generated as response of scan rate (mV/s), Inset (b) potential as function of scan rate.

### 5.5. Electrochemical response studies:

The response of the BSA/anti-CYFRA-21-1/APTES/$HfO_2$/ITO immunoelectrode has been investigated as a function of antigen concentration using CV **(Figure 10)**. The response studies have been carried out in PBS (pH 7.0) containing 5mM $[Fe(CN)_6]^{3-/4-}$ at a scan rate of 50 mV/s in the potential range -0.8 to 0.8V. The immunoelectrode is incubated with antigen solution for 15 minutes for antigen-antibody interaction prior to the CV measurements. It is observed that the electrochemical peak current gradually decreases linearly with increased concentration of CYFRA-21-1 **(inset b in Figure 10)**. The decreased current is attributed to the formation of electrically insulating antigen-antibody complex that may obstruct the electron transfer through $[Fe(CN)_6]^{3-/4-}$ redox conversion. The obtained calibration curve between peak current and antigen concentrations obey the following linear equation (viii)

$$I_{pa} = [\ 2.32\ (\mu A\ mL\ ng^{-1}\ ) \times \text{concentration of CYFRA-21-1 } (ng\ mL^{-1}) - 0.334\ \mu A], \quad R^2=0.988 \quad \ldots\ldots(viii)$$

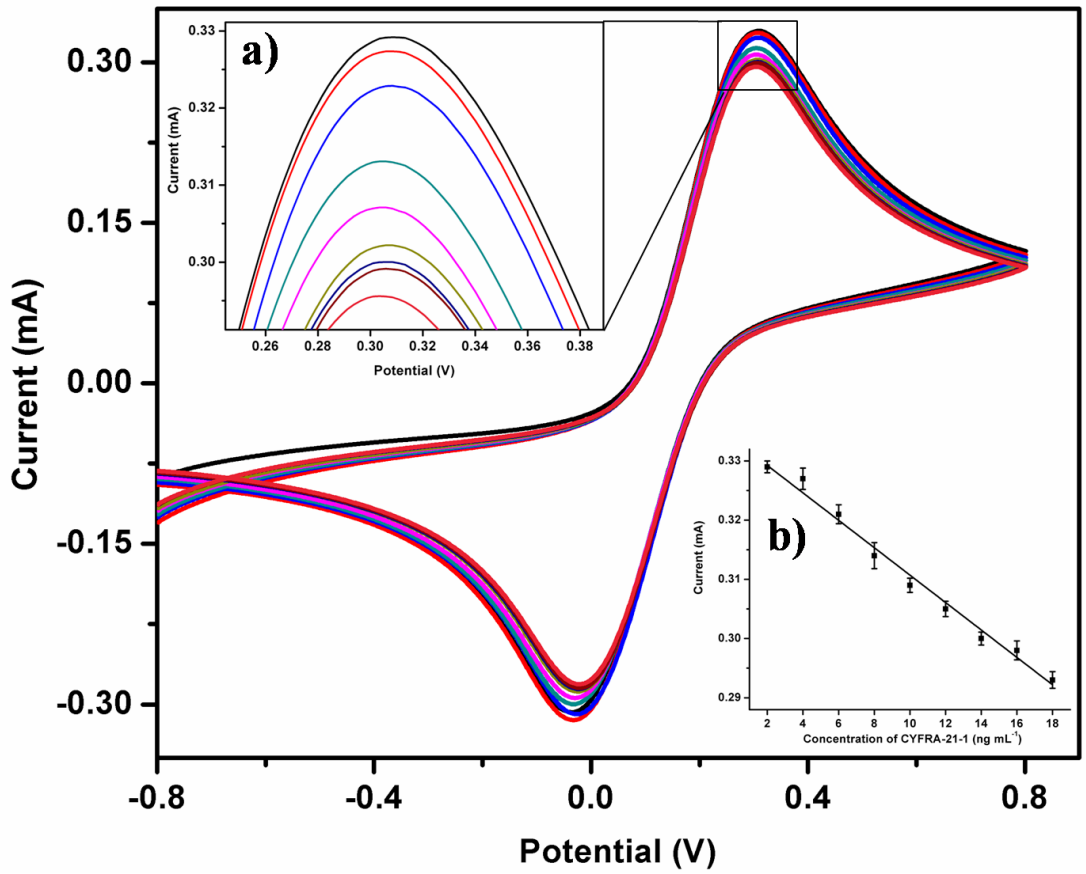


**Figure 10.** Electrochemical response of BSA/anti-CYFRA-21-1/APTES/$HfO_2$/ITO immunoelectrode as a function of CYFRA-21-1 concentration (2 ng $mL^{-1}$ to 18 ng $mL^{-1}$). The magnified view of oxidation peak current (inset a), calibration curve between magnitude of peak current and concentration of CYFRA-21-1 (ng $mL^{-1}$) (inset b).

**Figure 10. (inset b)** reveals that linearity is obtained in between 2 to 18 ng $mL^{-1}$, sensitivity is 9.28 µA mL $ng^{-1}$ $cm^{-2}$ with regression coefficient ($R^2$) is 0.983 and the lower detection limit is 0.209 ng $mL^{-1}$. The repeatability of the fabricated immunoelectrode is upto 30 times after which the peak current rapidly decreases. The storage stability of the BSA/anti-CYFRA-21-1/APTES/$HfO_2$/ITO immunoelectrode has been determined by observing CV at regular intervals of time for 10 weeks. The immunoelectrode is stored at 4 °C when not in use.

**5.6. Control experiment and interferents study:** A control experiment was conducted using the APTES/$HfO_2$/ITO electrode under similar conditions **(Figure 11.)**. We did not observe any significant change in the current response of the electrode with increasing concentration of CYFRA-21-1. These results reveal that APTES/$HfO_2$/ITO electrode does not interact with the antigen molecules in absence of antibodies.

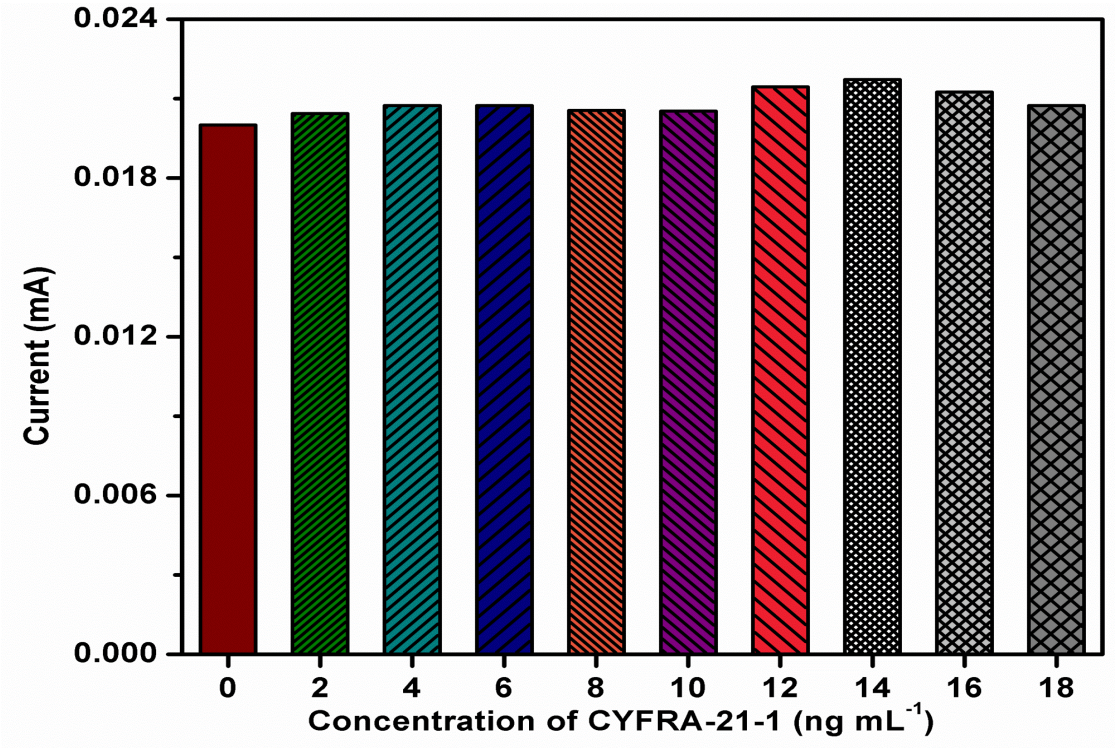


**Figure 11.** Control experiment (through electrochemical response study) of APTES/$HfO_2$/ITO electrode as a function of CYFRA-21-1 concentration (0-18ng $mL^{-1}$).

The BSA/anti-CYFRA-21-1/APTES/$HfO_2$/ITO immunoelectrode is pre-incubated with different interfering species present in human saliva such as carcino embronic antigen (CEA) (concentration 4-16 ng $mL^{-1}$), cardiac troponine I (Tn-I) (concentration: 0.19 ng $mL^{-1}$), sodium carboxymethyl cellulose (NaCMC) (concentration: 10 g $L^{-1}$) and glucose (7 mg $mL^{-1}$). The current response of immunoelectrode in the presence of these interferents has been shown in **Figure 12**. No significant change in current is observed due to addition of the interfering species. On the other hand, the peak current is found to be reduced after addition of CYFRA-21-1 (2 ng $mL^{-1}$) indicating that the BSA/anti-CYFRA-21-1/APTES/$HfO_2$/ITO immunoelectrode specifically interacts with CYFRA-21-1 and the response is not affected due to the presence of potential interferents present in saliva.

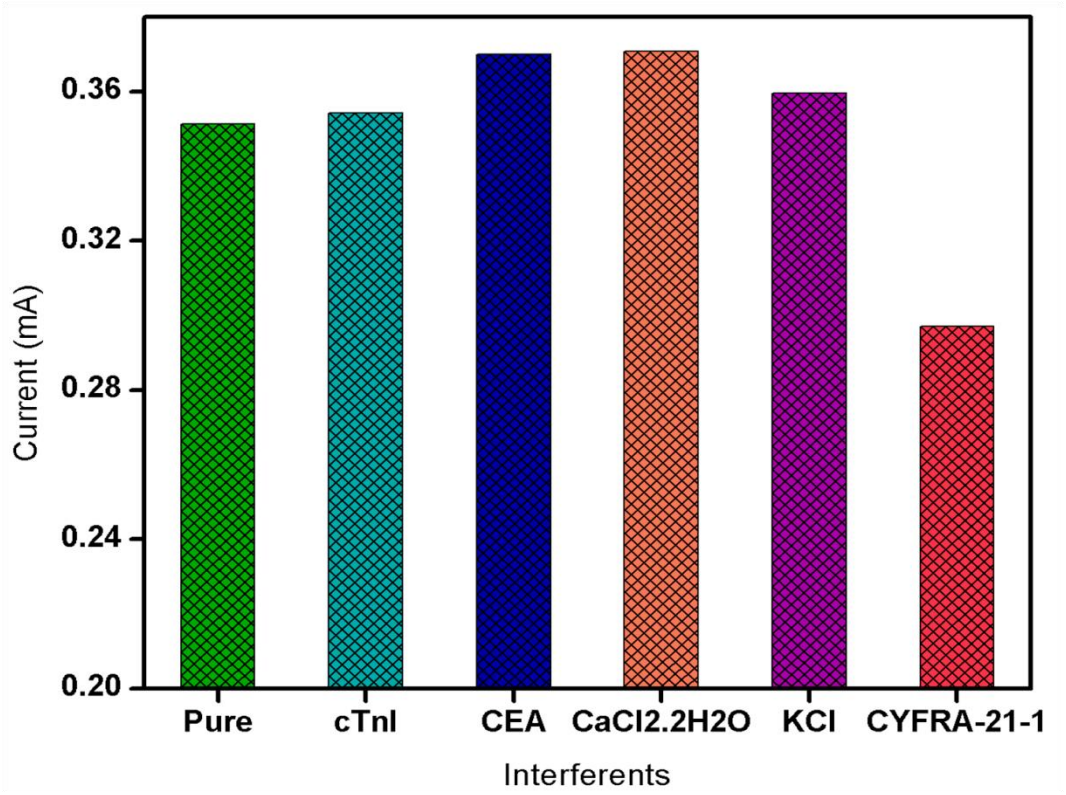


**Figure 12.** Interferents studies of BSA/anti-CYFRA-21-1/APTES/$HfO_2$/ITO immunoelectrode

### 5.7. Real sample analysis:

We have taken saliva sample of ten oral cancer patients for determination of CYFRA-21-1 antigen. Sample is processed as discussed earlier and analyzed through standard enzyme linked immune- sorbent assay (ELISA) techniques. We have quantified the concentration of CYFRA-21-1 through double-antibody sandwich ELISA kit (KinesisDX, USA) in triplicate. The microtiter wells are pre-coated with anti-CYFRA-21-1. After following all the steps, colorimetric reaction occurs and the absorbance is recorded at 450 nm in ELISA plate reader. A series of CYFRA-21-1 concentration in saliva samples obtained by ELISA were used to test the accuracy of the fabricated biosensor. The current response recorded for these real samples, matches with the current obtained for standard samples of the same concentration. We observe excellent correlation between the current obtained for real sample and standard sample concentrations (**Figure 13.**). The obtained results exhibit acceptable %RSD (relative standard deviation) indicating high accuracy of the fabricated biosensor.

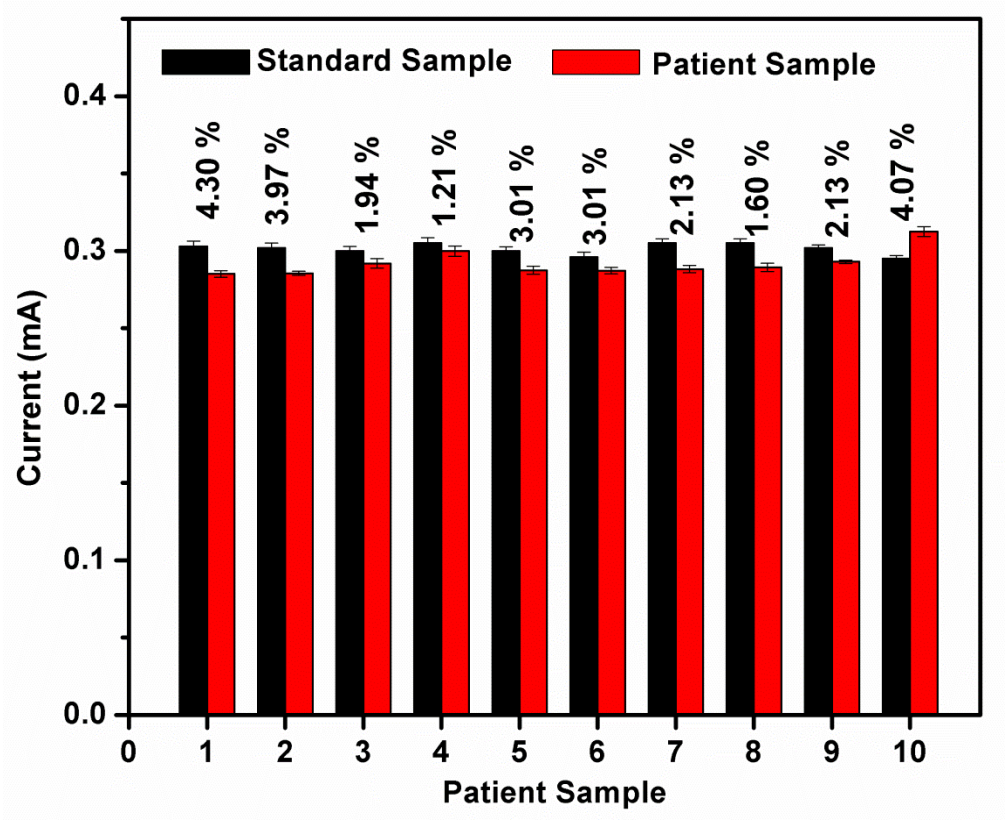


**Figure 13.** Comparative analysis of current response between standard sample and patient samples through fabricated BSA/anti-CYFRA-21-1/APTES/$HfO_2$/ITO immunoelectrode.

**5.8. Shelf-life study:** The shelf-life of BSA/anti-CYFRA-21-1/APTES/$HfO_2$/ITO immunoelectrode has been estimated by CV response in standard solution of PBS (pH 7.0, 0.9% NaCl) containing 5mM $[Fe(CN)_6]^{3-/4-}$ at one week interval. The weekly study of the immunoelectrode showed no significant change (**Figure. 5.13**) in peak current up to eight weeks, after which decrease in the peak current is observed.

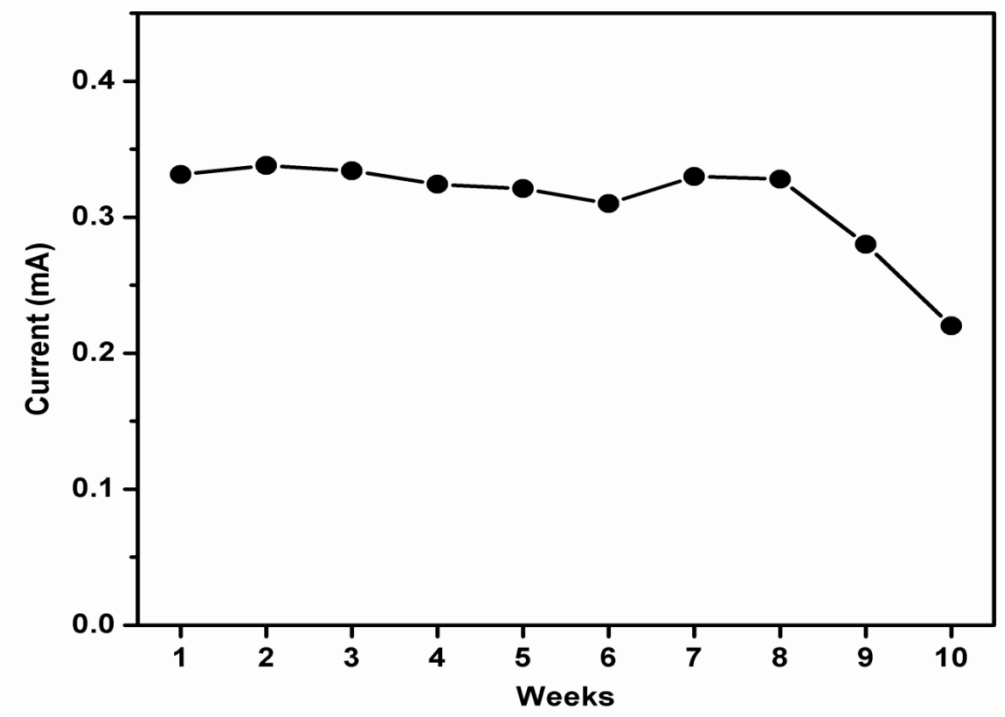


**Figure 14.** Shelf life studies of BSA/anti-CYFRA-21-1/APTES/$HfO_2$/ITO immunoelectrode

| Method | Detection Technique | Invasive/ Non-invasive | Label | Sample | Biomarker | Concentration range of biomarker | Detection Parameter | Response time | Ref. |
|---|---|---|---|---|---|---|---|---|---|
| **Cytopathology** | Staining | Invasive | ----- | Cells | ----- | ----- | ----- | 1 week | (Rosenberg and Cretin 1989) |
| **Biopsy** | Cell culture | Invasive | ------ | Tissue | ------ | ------ | ------ | 2-3 weeks | (Patton et al. 2008) |
| **Visualization adjuncts** | Staining | Invasive | ------ | Tissue | ------ | ------ | ------ | 1 week | (Patton et al. 2008) |
| **Biosensor** | Amperometric | Invasive | Yes | Serum | IL-6 (Protein) | ≤6 pg $mL^{-1}$ to ≥20 pg $mL^{-1}$ | S: 19.3 nA-mL (pg IL-6)$^{-1}$ $cm^{-2}$<br>LDR: 0.5–30 pg $mL^{-1}$<br>SL:---- | ----- | (Malhotra et al. 2010) |
| | Differential pulse voltammetry | Invasive | Yes | Serum | IL-6 (Protein) | <6 pg $mL^{-1}$ to >20 pg $mL^{-1}$ | S:----<br>LDR: 0.002-20 ng $mL^{-1}$<br>SL: One month | ------ | (Li and Yang 2011) |
| | Chrono-amperometry | Non Invasive | Yes | Saliva | has-miR-200a ( mi-RNA) | ------ | S:----<br>LDR: 1aM-10fM<br>SL:---- | ------ | (Wang et al. 2013a) |
| | Cyclic Voltammetry | Non Invasive | No | Saliva | CYFRA-21-1 (Protein) | 0-18 ng $mL^{-1}$ | S: 2.2 µA mL $ng^{-1}$<br>LDR: 2-16 ng $mL^{-1}$<br>SL: 6 weeks | 20 min | (Suveen Kumar) |
| | Cyclic Voltammetry | Non Invasive | No | Saliva | CYFRA-21-1 (Protein) | 0-18 ng $mL^{-1}$ | S: 9.28 µA mL $ng^{-1}$ $cm^{-2}$<br>LDR: 2-18 ng $mL^{-1}$<br>SL: 8 weeks | 15 min | Present Work |

S= Sensitivity, LDR= Linear detection range, SL= Shelf life

**Table 2.** Characteristics of the various detection techniques used for OC detection.

# Chapter-6

# Conclusions

In conclusion, the functionalized hafnium oxide nanoparticles have been utilized for fabrication of a label free, non-invasive and efficient immunosensor for oral cancer detection. $HfO_2$ nanoparticles have been synthesized via hydrothermal method and functionalized through APTES. Thin films of APTES/$HfO_2$/ITO have been fabricated using electrophoretic deposition method that has been biofunctionalized with the antibodies. Results of the studies indicate that the fabricated BSA/anti-CYFRA-21-1/APTES/$HfO_2$/ITO immunoelectrode has good linearity, in the range, 2 to 18 ng $mL^{-1}$ (with regression coefficient = 0.988), sensitivity of 9.28 μA mL $ng^{-1}$ $cm^{-2}$, and lower detection limit of 0.209 ng $mL^{-1}$. The shelf life of the immunoelectrode is 8 weeks and is reusable upto 30 times. Efforts should be made to utilize hafnium oxide based platform for detection of other cancer biomarkers.

# Chapter-7

# Future perspectives

The experimental investigations reveal that the hafnium oxide ($MO_x$) can be utilized in the development of high performance electrochemical biosensing devices with high sensitivity, selectivity, stability and design flexibility for laboratory applications.

Since the introduction of microfluidics technology in the early 1990s, an enormous amount of effort has been conducted towards the development of microfluidic immunosensors that combine the analytical power of microfluidic devices with the high specificity of antibody–antigen interactions. Recently, the microfluidics technology coupled with nanoscience and nanotechnology are becoming powerful tools in biosensors fabrication, due to the advantages of high performance, design flexibility, reagent economy, high throughput, miniaturization, and automation. These miniaturized chip devices can notably change the speed and scale towards highly specific and selective antibody–antigen interactions. Attributing to the interesting physiochemical properties of the $MO_x$s, it would be interesting to incorporate $MO_x$s and there derivative in microfluidic devices which would further open a new area of research and probably meet the real challenge in high performance biosensing. It is anticipated that the microfluidic biosensors based on these $MO_x$s will soon lead to decisive improvements in quality of human life. It should be interesting to fabricate some of the $MO_x$s based biosensors for application in clinical diagnostics.

# Chapter-8

# References

Ali, M.A., Srivastava, S., Solanki, P.R., Reddy, V., Agrawal, V.V., Kim, C., John, R., Malhotra, B.D., 2013. Highly efficient bienzyme functionalized nanocomposite-based microfluidics biosensor platform for biomedical application. Scientific reports 3.
Ambrosi, A., Airo, F., Merkoçi, A., 2009. Enhanced gold nanoparticle based ELISA for a breast cancer biomarker. Analytical chemistry 82(3), 1151-1156.
Arya, S.K., Bhansali, S., 2011. Lung cancer and its early detection using biomarker-based biosensors. Chemical reviews 111(11), 6783-6809.
Bahar, G., Feinmesser, R., Shpitzer, T., Popovtzer, A., Nagler, R.M., 2007. Salivary analysis in oral cancer patients. Cancer 109(1), 54-59.
Brailo, V., Vučićević-Boras, V., Cekić-Arambašin, A., Alajbeg, I., Milenović, A., Lukač, J., 2006. The significance of salivary interleukin 6 and tumor necrosis factor alpha in patients with oral leukoplakia. Oral oncology 42(4), 370-373.
Brocklehurst, P., Kujan, O., O'Malley, L.A., Ogden, G., Shepherd, S., Glenny, A.M., 2013. Screening programmes for the early detection and prevention of oral cancer. Cochrane Database Syst Rev 11.
Cady, N.C., Fahrenkopf, N., Mosier, A., 2009. Novel approaches to biosensing and nano-biological interactions. SPIE NanoScience+ Engineering, pp. 739707-739707-739707. International Society for Optics and Photonics.
Chaubey, G.S., Yao, Y., Makongo, J.P., Sahoo, P., Misra, D., Poudeu, P.F., Wiley, J.B., 2012. Microstructural and thermal investigations of HfO 2 nanoparticles. RSC Advances 2(24), 9207-9213.
Chen, J., Zhang, J., Guo, Y., Li, J., Fu, F., Yang, H.-H., Chen, G., 2011. An ultrasensitive electrochemical biosensor for detection of DNA species related to oral cancer based on nuclease-assisted target recycling and amplification of DNAzyme. Chemical Communications 47(28), 8004-8006.
Chen, Y.W., Liu, M., Kaneko, T., McIntyre, P.C., 2010. Atomic layer deposited hafnium oxide gate dielectrics for charge-based biosensors. Electrochemical and Solid-State Letters 13(3), G29-G32.
Crist, B.V., 2000. Handbook of monochromatic XPS spectra, The elements of native Oxides. Handbook of Monochromatic XPS Spectra, The Elements of Native Oxides, by B. Vincent Crist, pp. 548. ISBN 0-471-49265-5. Wiley-VCH, October 2000. 1.
Das, M., Dhand, C., Sumana, G., Srivastava, A., Vijayan, N., Nagarajan, R., Malhotra, B., 2011. Zirconia grafted carbon nanotubes based biosensor for M. Tuberculosis detection. Applied Physics Letters 99(14), 143702.
De Jong, E.P., Xie, H., Onsongo, G., Stone, M.D., Chen, X.-B., Kooren, J.A., Refsland, E.W., Griffin, R.J., Ondrey, F.G., Wu, B., 2010. Quantitative proteomics reveals myosin and actin as promising saliva biomarkers for distinguishing pre-malignant and malignant oral lesions. PLoS One 5(6), e11148.
De Vos, W., Casselman, J., Swennen, G., 2009. Cone-beam computerized tomography (CBCT) imaging of the oral and maxillofacial region: a systematic review of the literature. International journal of oral and maxillofacial surgery 38(6), 609-625.
Deng, C., Zhang, X., Li, N., 2004. Investigation of volatile biomarkers in lung cancer blood using solid-phase microextraction and capillary gas chromatography–mass spectrometry. Journal of Chromatography B 808(2), 269-277.
Doweck, I., Barak, M., Greenberg, E., Uri, N., Kellner, J., Lurie, M., Gruener, N., 1995. Cyfra 21-1: A new potential tumor marker for squamous cell carcinoma of head and neck. Archives of Otolaryngology–Head & Neck Surgery 121(2), 177-181.
El-Sayed, I.H., Huang, X., El-Sayed, M.A., 2005. Surface plasmon resonance scattering and absorption of anti-EGFR antibody conjugated gold nanoparticles in cancer diagnostics: applications in oral cancer. Nano letters 5(5), 829-834.

Eliziário, S., Cavalcante, L., Sczancoski, J., Pizani, P., Varela, J.A., Espinosa, J., Longo, E., 2009. Morphology and photoluminescence of HfO2 obtained by microwave-hydrothermal. Nanoscale research letters 4(11), 1371-1379.
Fahrenkopf, N.M., Oktyabrsky, S., Eisenbraun, E., Bergkvist, M., Shi, H., Cady, N.C., 2009. Phosphate-dependent DNA Immobilization on Hafnium Oxide for Bio-Sensing Applications. MRS Proceedings, pp. 1191-OO1112-1104. Cambridge Univ Press.
Fahrenkopf, N.M., Rice, P.Z., Bergkvist, M., Deskins, N.A., Cady, N.C., 2012. Immobilization Mechanisms of Deoxyribonucleic Acid (DNA) to Hafnium Dioxide (HfO2) Surfaces for Biosensing Applications. ACS applied materials & interfaces 4(10), 5360-5368.
Farah, C., Vu, A., Allen, K., McCullough, M., Ford, P., 2012. Oral cancer and potentially cancerous lesions-early detection and diagnosis. INTECH Open Access Publisher.
Fedele, S., 2009. Diagnostic aids in the screening of oral cancer. Head & neck oncology 1(1), 5.
Fend, F., Raffeld, M., 2000. Laser capture microdissection in pathology. Journal of clinical pathology 53(9), 666-672.
Firth, N., 1997. Marijuana use and oral cancer: a review. Oral oncology 33(6), 398-401.
Giannobile, W.V., Beikler, T., Kinney, J.S., Ramseier, C.A., Morelli, T., Wong, D.T., 2009. Saliva as a diagnostic tool for periodontal disease: current state and future directions. Periodontology 2000 50(1), 52-64.
Gorschinski, A., Khelashvili, G., Schild, D., Habicht, W., Brand, R., Ghafari, M., Bönnemann, H., Dinjus, E., Behrens, S., 2009. A simple aminoalkyl siloxane-mediated route to functional magnetic metal nanoparticles and magnetic nanocomposites. Journal of Materials Chemistry 19(46), 8829-8838.
Graham, S., Dayal, H., Rohrer, T., Swanson, M., Sultz, H., Shedd, D., Fischman, S., 1977. Dentition, diet, tobacco, and alcohol in the epidemiology of oral cancer. Journal of the National Cancer Institute 59(6), 1611-1618.
Haeckel, R., Hanecke, P., 1996. Application of saliva for drug monitoring an in vivo model for transmembrane transport. European journal of clinical chemistry and clinical biochemistry 34(3), 171-192.
Herrero, R., Castellsagué, X., Pawlita, M., Lissowska, J., Kee, F., Balaram, P., Rajkumar, T., Sridhar, H., Rose, B., Pintos, J., 2003. Human papillomavirus and oral cancer: the International Agency for Research on Cancer multicenter study. Journal of the National Cancer Institute 95(23), 1772-1783.
Hu, S., Arellano, M., Boontheung, P., Wang, J., Zhou, H., Jiang, J., Elashoff, D., Wei, R., Loo, J.A., Wong, D.T., 2008. Salivary proteomics for oral cancer biomarker discovery. Clinical Cancer Research 14(19), 6246-6252.
Jou, Y.-J., Lin, C.-D., Lai, C.-H., Chen, C.-H., Kao, J.-Y., Chen, S.-Y., Tsai, M.-H., Huang, S.-H., Lin, C.-W., 2010. Proteomic identification of salivary transferrin as a biomarker for early detection of oral cancer. Analytica chimica acta 681(1), 41-48.
Kademani, D., 2007. Oral cancer. Mayo Clinic Proceedings, pp. 878-887. Elsevier.
Kidchob, T., Malfatti, L., Serra, F., Falcaro, P., Enzo, S., Innocenzi, P., 2007. Hafnium oxide sol-gel films synthesized from HfCl4: Changes of structure and properties with the firing temperature. Journal of sol-gel science and technology 42(1), 89-93.
Kujan, O., Glenny, A.M., Oliver, R., Thakker, N., Sloan, P., 2006. Screening programmes for the early detection and prevention of oral cancer. The Cochrane Library.
Kumar, S., Kumar, S., Ali, M., Anand, P., Agrawal, V.V., John, R., Maji, S., Malhotra, B.D., 2013. Microfluidic-integrated biosensors: Prospects for point-of-care diagnostics. Biotechnology journal 8(11), 1267-1279.
Kumar, S., Kumar, S., Tiwari, S., Srivastava, S., Srivastava, M., Yadav, B.K., Kumar, S., Tran, T.T., Dewan, A.K., Mulchandani, A., 2015. Biofunctionalized Nanostructured Zirconia

for Biomedical Application: A Smart Approach for Oral Cancer Detection. Advanced Science.
Kumar, S., Singh, J., Agrawal, V., Ahamad, M., Malhotra, B., 2011. Biocompatible self-assembled monolayer platform based on (3-glycidoxypropyl) trimethoxysilane for total cholesterol estimation. Analytical Methods 3(10), 2237-2245.
Lai, R.-S., Chen, C.-C., Lee, P.-C., Lu, J.-Y., 1999. Evaluation of cytokeratin 19 fragment (CYFRA 21-1) as a tumor marker in malignant pleural effusion. Japanese journal of clinical oncology 29(9), 421-424.
Lee, E.J., Ribeiro, C., Longo, E., Leite, E.R., 2006. Growth kinetics of tin oxide nanocrystals in colloidal suspensions under hydrothermal conditions. Chemical physics 328(1), 229-235.
Lee, M., Zine, N., Baraket, A., Zabala, M., Campabadal, F., Caruso, R., Trivella, M.G., Jaffrezic-Renault, N., Errachid, A., 2012. A novel biosensor based on hafnium oxide: Application for early stage detection of human interleukin-10. Sensors and Actuators B: Chemical 175, 201-207.
Lee, Y.-H., Wong, D.T., 2009. Saliva: an emerging biofluid for early detection of diseases. American journal of dentistry 22(4), 241.
Lestón, J.S., Dios, P.D., 2010. Diagnostic clinical aids in oral cancer. Oral oncology 46(6), 418-422.
Li, T., Yang, M., 2011. Electrochemical sensor utilizing ferrocene loaded porous polyelectrolyte nanoparticles as label for the detection of protein biomarker IL-6. Sensors and Actuators B: Chemical 158(1), 361-365.
Liu, G., Lin, Y., 2005. Electrochemical sensor for organophosphate pesticides and nerve agents using zirconia nanoparticles as selective sorbents. Analytical chemistry 77(18), 5894-5901.
Liu, L., Ma, Z., Xie, Y., Su, Y., Zhao, H., Zhou, M., Zhou, J., Li, J., Xie, E., 2010. Photoluminescence of rare earth 3+ doped uniaxially aligned HfO2 nanotubes prepared by sputtering with electrospun polyvinylpyrolidone nanofibers as templates. Journal of Applied Physics 107(2), 024309.
Llewellyn, C.D., Linklater, K., Bell, J., Johnson, N.W., Warnakulasuriya, S., 2004. An analysis of risk factors for oral cancer in young people: a case-control study. Oral oncology 40(3), 304-313.
Ludwig, J.A., Weinstein, J.N., 2005. Biomarkers in cancer staging, prognosis and treatment selection. Nature Reviews Cancer 5(11), 845-856.
Malathi, N., Mythili, S., Vasanthi, H.R., 2014. Salivary diagnostics: a brief review. ISRN dentistry 2014.
Malhotra, R., Patel, V., Chikkaveeraiah, B.V., Munge, B.S., Cheong, S.C., Zain, R.B., Abraham, M.T., Dey, D.K., Gutkind, J.S., Rusling, J.F., 2012. Ultrasensitive detection of cancer biomarkers in the clinic by use of a nanostructured microfluidic array. Analytical chemistry 84(14), 6249-6255.
Malhotra, R., Patel, V., Vaqué, J.P., Gutkind, J.S., Rusling, J.F., 2010. Ultrasensitive electrochemical immunosensor for oral cancer biomarker IL-6 using carbon nanotube forest electrodes and multilabel amplification. Analytical chemistry 82(8), 3118-3123.
Massano, J., Regateiro, F.S., Januário, G., Ferreira, A., 2006. Oral squamous cell carcinoma: review of prognostic and predictive factors. Oral Surgery, Oral Medicine, Oral Pathology, Oral Radiology, and Endodontology 102(1), 67-76.
Mehrotra, R., Gupta, A., Singh, M., Ibrahim, R., 2006. Application of cytology and molecular biology in diagnosing premalignant or malignant oral lesions. Molecular Cancer 5(1), 11.
Mehrotra, R., Gupta, D.K., 2011. Exciting new advances in oral cancer diagnosis: avenues to early detection. Head & neck oncology 3(1), 1-9.

Michael, L., Baraket, A., Nadia, Z., Zabala, M., Campabadal, F., Jaffrezic-Renault, N., 2014. Impedance Characterization of the Capacitive field-Effect pH-Sensor Based on a thin-Layer Hafnium Oxide Formed by Atomic Layer Deposition.
Mizukawa, N., Sugiyama, K., Fukunaga, J., Ueno, T., Mishima, K., Takagi, S., Sugahara, T., 1997. Defensin-1, a peptide detected in the saliva of oral squamous cell carcinoma patients. Anticancer research 18(6B), 4645-4649.
Nagler, R., Bahar, G., Shpitzer, T., Feinmesser, R., 2006. Concomitant analysis of salivary tumor markers—a new diagnostic tool for oral cancer. Clinical Cancer Research 12(13), 3979-3984.
Nagler, R.M., Barak, M., Peled, M., Ben-Aryeh, H., Filatov, M., Laufer, D., 1999. Early diagnosis and treatment monitoring roles of tumor markers Cyfra 21-1 and TPS in oral squamous cell carcinoma. Cancer 85(5), 1018-1025.
Nagler, R.M., Hershkovich, O., Lischinsky, S., Diamond, E., Reznick, A.Z., 2002. Saliva analysis in the clinical setting: revisiting an underused diagnostic tool. Journal of investigative medicine 50(3), 214-225.
Pan, T.-M., Huang, M.-D., Lin, C.-W., Wu, M.-H., 2010. Development of high-κ HoTiO 3 sensing membrane for pH detection and glucose biosensing. Sensors and Actuators B: Chemical 144(1), 139-145.
Patton, L.L., Epstein, J.B., Kerr, A.R., 2008. Adjunctive techniques for oral cancer examination and lesion diagnosis: a systematic review of the literature. The Journal of the American Dental Association 139(7), 896-905.
Pickering, V., Jordan, R.C., Schmidt, B.L., 2007. Elevated salivary endothelin levels in oral cancer patients—a pilot study. Oral oncology 43(1), 37-41.
Proia, N.K., Paszkiewicz, G.M., Nasca, M.A.S., Franke, G.E., Pauly, J.L., 2006. Smoking and smokeless tobacco-associated human buccal cell mutations and their association with oral cancer—a review. Cancer Epidemiology Biomarkers & Prevention 15(6), 1061-1077.
Rajkumar, K., Ramya, R., Nandhini, G., Rajashree, P., Ramesh Kumar, A., Nirmala Anandan, S., 2015. Salivary and serum level of CYFRA 21-1 in oral precancer and oral squamous cell carcinoma. Oral diseases 21(1), 90-96.
Rhodus, N., Cheng, B., Bowles, W., Myers, S., Miller, L., Ondrey, F., 2006. Proinflammatory cytokine levels in saliva before and after treatment of (erosive) oral lichen planus with dexamethasone. Oral diseases 12(2), 112-116.
Rosenberg, D., Cretin, S., 1989. Use of meta-analysis to evaluate tolonium chloride in oral cancer screening. Oral Surgery, Oral Medicine, Oral Pathology 67(5), 621-627.
Santarelli, A., Mascitti, M., Lo Russo, L., Colella, G., Giannatempo, G., 2013. Detection Level of Salivary Survivin in Patients with OSCC. J Carcinogene Mutagene S 5, 29-85.
Scully, C., Bagan, J.V., Hopper, C., Epstein, J.B., 2008. Oral cancer: current and future diagnostic techniques. Am J Dent 21(4), 199-209.
Shim, J., Rivera, J.A., Bashir, R., 2013. Electron beam induced local crystallization of HfO 2 nanopores for biosensing applications. Nanoscale 5(22), 10887-10893.
Shpitzer, T., Hamzany, Y., Bahar, G., Feinmesser, R., Savulescu, D., Borovoi, I., Gavish, M., Nagler, R., 2009. Salivary analysis of oral cancer biomarkers. British journal of cancer 101(7), 1194-1198.
Silverman, S., 2003. Oral cancer. PMPH-USA.
Singh, C., Srivastava, S., Ali, M.A., Gupta, T.K., Sumana, G., Srivastava, A., Mathur, R., Malhotra, B.D., 2013. Carboxylated multiwalled carbon nanotubes based biosensor for aflatoxin detection. Sensors and Actuators B: Chemical 185, 258-264.
Singh, J., Srivastava, M., Roychoudhury, A., Lee, D.W., Lee, S.H., Malhotra, B., 2012. Bienzyme-functionalized monodispersed biocompatible cuprous oxide/chitosan nanocomposite platform for biomedical application. The Journal of Physical Chemistry B 117(1), 141-152.

Solanki, P.R., Kaushik, A., Agrawal, V.V., Malhotra, B.D., 2011. Nanostructured metal oxide-based biosensors. NPG Asia Materials 3(1), 17-24.
Stieber, P., Hasholzner, U., Bodenmüller, H., Nagel, D., Sunder-Plassmann, L., Dienemann, H., Meier, W., Fateh-Moghadam, A., 1993. CYFRA 21-1: A new marker in lung cancer. Cancer 72(3), 707-713.
Streckfus, C., Bigler, L., 2002. Saliva as a diagnostic fluid. Oral diseases 8(2), 69-76.
Suveen Kumar, S.K., Sachchidanand Tiwari, Saurabh Srivastava, Manish Srivastava, Birendra Kumar Yadav, Saroj Kumar, Thien Toan Tran, Ajay Kumar Dewan, Ashok Mulchandani, Jai Gopal Sharma, Sagar Maji and Bansi Dhar Malhotra, Biofunctionalized Nanostructured Zirconia for Biomedical Application: A Smart Approach for Oral Cancer Detection. Advanced Science Communicated.
Tan, W., Sabet, L., Li, Y., Yu, T., Klokkevold, P.R., Wong, D.T., Ho, C.-M., 2008. Optical protein sensor for detecting cancer markers in saliva. Biosensors and Bioelectronics 24(2), 266-271.
Vasudev, A., Kaushik, A., Bhansali, S., 2013. Electrochemical immunosensor for label free epidermal growth factor receptor (EGFR) detection. Biosensors and Bioelectronics 39(1), 300-305.
Wang, C.-Y., Chiang, H.K., Chen, C.-T., Chiang, C.-P., Kuo, Y.-S., Chow, S.-N., 1999. Diagnosis of oral cancer by light-induced autofluorescence spectroscopy using double excitation wavelengths. Oral oncology 35(2), 144-150.
Wang, J.-H., Wang, B., Liu, Q., Li, Q., Huang, H., Song, L., Sun, T.-Y., Wang, H., Yu, X.-F., Li, C., 2013a. Bimodal optical diagnostics of oral cancer based on Rose Bengal conjugated gold nanorod platform. Biomaterials 34(17), 4274-4283.
Wang, J., 2006. Electrochemical biosensors: towards point-of-care cancer diagnostics. Biosensors and Bioelectronics 21(10), 1887-1892.
Wang, Z., Zhang, J., Guo, Y., Wu, X., Yang, W., Xu, L., Chen, J., Fu, F., 2013b. A novel electrically magnetic-controllable electrochemical biosensor for the ultra sensitive and specific detection of attomolar level oral cancer-related microRNA. Biosensors and Bioelectronics 45, 108-113.
Warnakulasuriya, S., Soussi, T., Maher, R., Johnson, N., Tavassoli, M., 2000. Expression of p53 in oral squamous cell carcinoma is associated with the presence of IgG and IgA p53 autoantibodies in sera and saliva of the patients. The Journal of pathology 192(1), 52-57.
Wei, F., Patel, P., Liao, W., Chaudhry, K., Zhang, L., Arellano-Garcia, M., Hu, S., Elashoff, D., Zhou, H., Shukla, S., 2009. Electrochemical sensor for multiplex biomarkers detection. Clinical Cancer Research 15(13), 4446-4452.
Wong, D.T., 2006. Salivary diagnostics powered by nanotechnologies, proteomics and genomics. The Journal of the American Dental Association 137(3), 313-321.
Yang, C.-Y., Brooks, E., Li, Y., Denny, P., Ho, C.-M., Qi, F., Shi, W., Wolinsky, L., Wu, B., Wong, D.T., 2005. Detection of picomolar levels of interleukin-8 in human saliva by SPR. Lab on a Chip 5(10), 1017-1023.
Yoshizawa, J.M., Schafer, C.A., Schafer, J.J., Farrell, J.J., Paster, B.J., Wong, D.T., 2013. Salivary biomarkers: toward future clinical and diagnostic utilities. Clinical microbiology reviews 26(4), 781-791.
Zangar, R.C., Daly, D.S., White, A.M., 2006. ELISA microarray technology as a high-throughput system for cancer biomarker validation. Expert Review of Proteomics 3(1), 37-44.
Zhao, M., Rosenbaum, E., Carvalho, A.L., Koch, W., Jiang, W., Sidransky, D., Califano, J., 2005. Feasibility of quantitative PCR-based saliva rinse screening of HPV for head and neck cancer. International journal of cancer 117(4), 605-610.
Zhong, L.-P., Chen, G.-F., Xu, Z.-F., Zhang, X., Ping, F.-Y., Zhao, S.-F., 2005. Detection of telomerase activity in saliva from oral squamous cell carcinoma patients. International journal of oral and maxillofacial surgery 34(5), 566-570.

Zimmermann, B.G., Wong, D.T., 2008. Salivary mRNA targets for cancer diagnostics. Oral oncology 44(5), 425-429.
Zini, A., Czerninski, R., Sgan-Cohen, H.D., 2010. Oral cancer over four decades: epidemiology, trends, histology, and survival by anatomical sites. Journal of oral pathology & medicine 39(4), 299-305.
Ziober, B.L., Mauk, M.G., Falls, E.M., Chen, Z., Ziober, A.F., Bau, H.H., 2008. Lab-on-a-chip for oral cancer screening and diagnosis. Head & neck 30(1), 111-121.